

# A Chemical Tuned Strategy to Develop Novel Irreversible EGFR-TK Inhibitors with Improved Safety and Pharmacokinetic Profiles

Guangxin Xia,<sup>‡,||</sup> Wenteng Chen,<sup>†,||</sup> Jing Zhang,<sup>‡</sup> Jian Shao,<sup>†</sup> Yong Zhang,<sup>‡</sup> Wei Huang,<sup>†</sup> Leduo Zhang,<sup>‡</sup> Weixing Qi,<sup>†</sup> Xing Sun,<sup>‡</sup> Bojun Li,<sup>‡</sup> Zhixiong Xiang,<sup>‡</sup> Chen Ma,<sup>‡</sup> Jia Xu,<sup>‡</sup> Hailin Deng,<sup>‡</sup> Yufeng Li,<sup>‡</sup> Ping Li,<sup>‡</sup> Hong Miao,<sup>‡</sup> Jiansheng Han,<sup>‡</sup> Yanjun Liu,<sup>‡</sup> Jingkang Shen,<sup>\*,‡,§</sup> and Yongping Yu<sup>\*,†</sup>

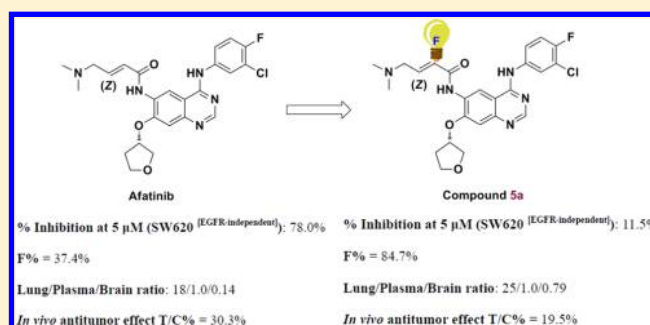
<sup>†</sup>Zhejiang Province Key Laboratory of Anti-Cancer Drug Research, College of Pharmaceutical Science, Zhejiang University, 866 Yuhangtang Road Zijin Campus, Hangzhou 310058, China

<sup>‡</sup>Central Research Institute, Shanghai Pharmaceutical Holding Co., Ltd., Building 4, No. 898 Ha Lei Road, Zhangjiang Hi-Tech Park, Shanghai 201203, China

<sup>§</sup>State Key Laboratory of Drug Research, Shanghai Institute of Materia Medica, Chinese Academy of Sciences, No. 555 Zuchongzhi Road, Zhangjiang Hi-Tech Park, Shanghai 201203, China

## S Supporting Information

**ABSTRACT:** Gatekeeper T790 M mutation in EGFR is the most prevalent factor underlying acquired resistance. Acrylamide-bearing quinazoline derivatives are powerful irreversible inhibitors for overcoming resistance. Nevertheless, concerns about the risk of nonspecific covalent modification have motivated the development of novel cysteine-targeting inhibitors. In this paper, we demonstrate that fluoro-substituted olefins can be tuned to alter Michael addition reactivity. Incorporation of these olefins into the quinazoline templates produced potent EGFR inhibitors with improved safety and pharmacokinetic properties. A lead compound **5a** was validated against EGFR<sup>WT</sup>, EGFR<sup>T790M</sup> as well as A431 and H1975 cancer cell lines. Additionally, compound **5a** displayed a weaker inhibition against the EGFR-independent cancer cell line SW620 when compared with afatinib. Oral administration of **5a** at a dose of 30 mg/kg induced tumor regression in a murine-EGFR<sup>L858R/T790M</sup> driven H1975 xenograft model. Also, **5a** exhibited improved oral bioavailability and safety as well as favorable tissue distribution properties and enhanced brain uptake. These findings provide the basis of a promising strategy toward the treatment of NSCLC patients with drug resistance.



## INTRODUCTION

The ErbB family kinases play a crucial regulatory role associated with a variety of malignancies, making this protein family an attractive drug target.<sup>1–4</sup> Despite the demonstrated clinical efficacy of reversible EGFR-TKIs,<sup>5,6</sup> not all patients with cancer respond to such treatment. The short-lived clinical outcome is partly due to the acquired drug resistant mutations in EGFR, which affect roughly 50% of the treated population.<sup>7,8</sup> The elucidated resistance mechanisms may be circumvented by irreversible kinase inhibitors. These inhibitors all rely on an acrylamide electrophilic warhead that forms a covalent bond with a conserved cysteine residue in EGFR (Cys797). The results enable a greater occupancy of the ATP binding site than is found with the reversible inhibitors, thus providing the ability to prolong the time of exposure and circumvent drug resistance.<sup>9,10</sup> Afatinib, an irreversible EGFR-TKI, was approved by the FDA for the treatment of patients with metastatic NSCLC in 2013.<sup>11</sup> However, these irreversible kinase inhibitors all contain with a reactive “warhead” which can irreversibly bind to proteins other than the target, creating a toxicity burden.<sup>12</sup>

In this study, we sought to exploit novel irreversible EGFR inhibitors to overcome the problem of drug resistance and to reduce the risk of nonspecific covalent binding.<sup>13</sup> To this end, we focused on replacement of the acrylamide function by alternative and less reactive electrophiles. A novel quinazoline analogue bearing fluoro-substituted olefins was designed and synthesized. Their EGFR kinase inhibitory activity, in vitro antiproliferative effects as well as preliminary pharmacokinetic studies and in vivo antitumor efficacy were evaluated. Consequently some compounds with greater potency and superior safety index were identified. A lead compound **5a** was found to effectively inhibit EGFR<sup>WT</sup>, EGFR<sup>T790M</sup> as well as A431 and H1975 cancer cell lines. Oral administration of **5a** led to tumor regression in a murine-EGFR<sup>L858R/T790M</sup> driven H1975 xenograft model. Also, **5a** exhibited improved oral bioavailability, as well as favorable tissue distribution properties, increased safety index, and enhanced brain uptake. These

Received: July 1, 2014

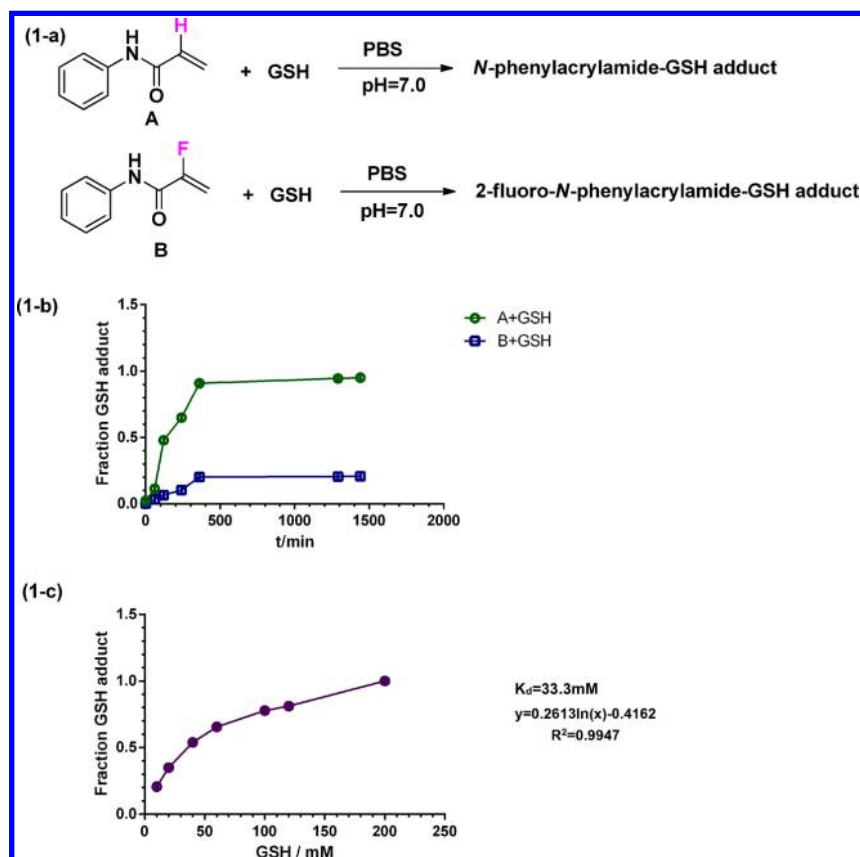


**Figure 1.** GSH conjugate addition to fluoro-substituted olefins. (1-a) model reaction between *N*-phenylacrylamide (A) or 2-fluoro-*N*-phenylacrylamide (B) and reduced GSH in PBS buffer. (1-b) Conjugate addition reactions of GSH (10 mM) with A (1 mM) or B (1 mM) at various time points (0–1440 min) and monitored by HPLC-HRMS. (1-c) B (1 mM) was treated with increasing concentrations of GSH (10–200 mM) and monitored by HPLC-HRMS.

findings provide a promising strategy for the development of novel treatments for NSCLC patients with drug resistance.

## RESULTS AND DISCUSSION

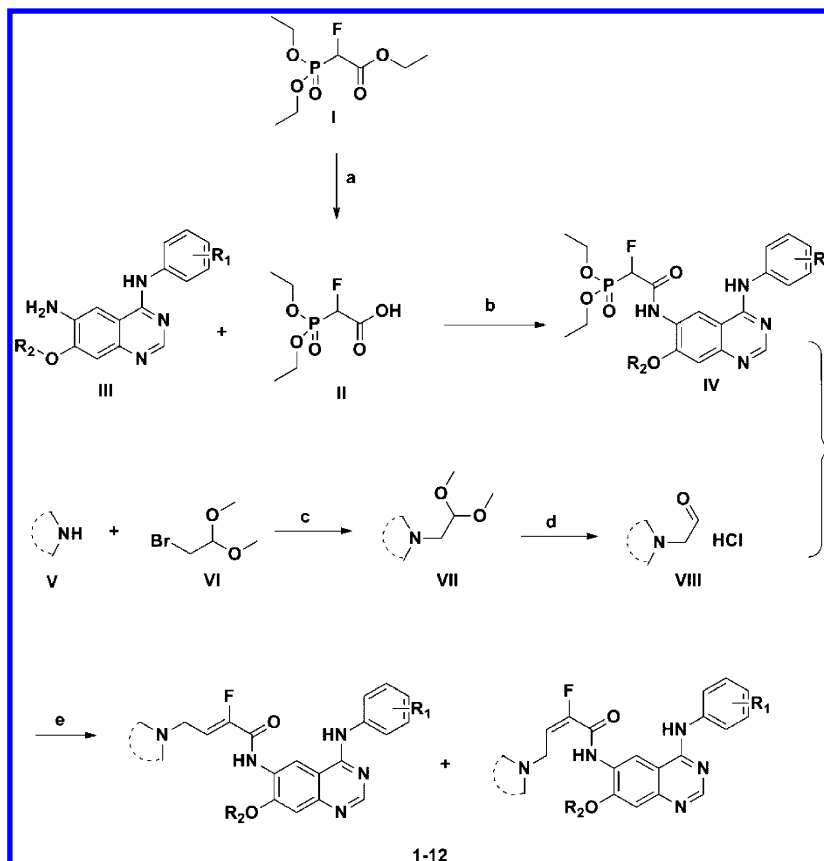
**Chemistry.** Attenuated electrophiles have a reduced likelihood of reacting irreversibly with off-target proteins.<sup>14a,b</sup> Because of the high electronegativity, small size, and special chemical reactivity with respect to hydrogen, we hypothesized the replacement of hydrogen at the  $\alpha$ -position of acrylamide with fluorine would chemically tune the Michael-type conjugate addition. To test this hypothesis, two simple Michael acceptors, *N*-phenylacrylamide (A) and 2-fluoro-*N*-phenylacrylamide (B), were synthesized and evaluated the Michael addition reaction rate with reduced glutathione (GSH) (Figure 1). Each compound was reacted separately with 10.0 equiv of GSH in PBS buffer at pH = 7.0, and the reactions were monitored by HPLC-HRMS. The results indicate that the conjugation reaction of A and GSH is significantly faster than that of B, with the production of the thioether adduct being 95.4% and 20.7%, respectively (Figure 1). Increasing concentrations of GSH was found to cause a stepwise decrease in the prominent UV–visible absorption band of B ( $\lambda = 214 \text{ nm}$ ). Fitting the titration data provides an apparent  $k_d$  of 33.3 mM (Figure 1-c). We anticipated that the slower model reaction between GSH and B would possibly result in less nonspecific covalent modification during binding to target proteins.<sup>14c</sup> Also, incorporation of fluorine into small molecules has been previously employed to optimize drug-like properties, such as

changes in cell uptake, tissue distribution, metabolic stability, and improved pharmacokinetic properties.<sup>15–18</sup> Consequently, we focused our efforts on the development of the fluoro-substituted olefin as a novel cysteine capture group.

Using a structure-based approach, quinazoline analogues bearing different geometric  $\alpha$ -fluoro acrylamides were designed and synthesized. Scheme 1 depicts the synthetic route for compounds 1–12. Compounds IV are synthesized by coupling their precursor amines (III) with the desired carboxylic acid (II). 6-Amino-4-anilinoquinazoline (III) is prepared in six steps from commercially available 2-amino-4-fluorobenzoic acid as previously reported.<sup>19,20</sup> The selective hydrolysis of phosphate (I) affords the corresponding 2-(diethoxyphosphoryl)-2-fluoroacetic acid (II) in excellent yield.<sup>21</sup> A Horner–Wadsworth–Emmons olefination of the quinazoline intermediates (IV) and the substituted aldehydes (VIII) provides a mixture of isomers (1–12) in good yield.<sup>22</sup> The corresponding aldehydes are prepared in two steps from secondary amines (V) by substitution with 2-bromo-1,1-dimethoxyethane (VI) and deprotection of the acetal in conc HCl.<sup>23</sup> The isomers (1–12) were separated by semiprep HPLC or Thar SFC Pre80 for biological testing.

Compound 5a was selected to react with GSH under physiological conditions for 120 min (Figure 2). In comparison to afatinib, compound 5a produced the conjugate adduct slowly, only 3% of thioether was detected (afatinib: 66.5%). This result revealed that compound 5a reacted more slowly with the thiol of GSH, potentially minimizing its chemical reactivity toward nonspecific targets.

Scheme 1. Synthesis of Compounds 1–12



<sup>a</sup>Conditions and reagents: (a) NaOH, EtOH, 0–5 °C; (b) (COCl<sub>2</sub>), Et<sub>3</sub>N, DCM/DMF, 0 °C–rt; (c) K<sub>2</sub>CO<sub>3</sub>, DMF, 90 °C; (d) conc HCl, reflux; (e) NaOH, EtOH–H<sub>2</sub>O, rt.

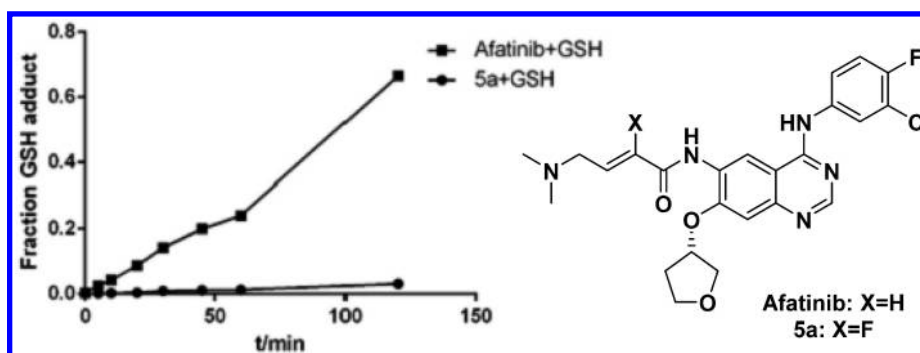
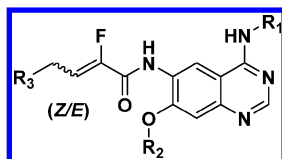


Figure 2. GSH conjugate addition of afatinib or compound 5a.

**Biological Evaluation.** To determine the *in vitro* potency, compounds 1–12 were screened against wild-type EGFR, T790 M mutant EGFR, and HER2. Significant potency differences were observed among the compounds 1–12, with distinct patterns of inhibition noted for the two types of EGFR kinases (IC<sub>50</sub> values range from 0.18 to 59.8 nM) (Table 1). The biological assay results show some differences in activity based on the geometric arrangement of the analogues. For instance, the IC<sub>50</sub> values for compounds 5a and 5b on EGFR<sup>T790M</sup> were 5.52 and 25.8 nM, respectively. The same trend was observed for 4a/4b (4a, 21.3 nM; 4b, 42.9 nM). The *trans*-isomers displayed more potent than the *cis*-isomers in the EGFR<sup>T790M</sup> kinase assay. On the other hand, the profile against HER2 shows that quinazoline analogues bearing  $\alpha$ -fluoro acrylamide are 2.5–89-fold less potent than afatinib (IC<sub>50</sub> =

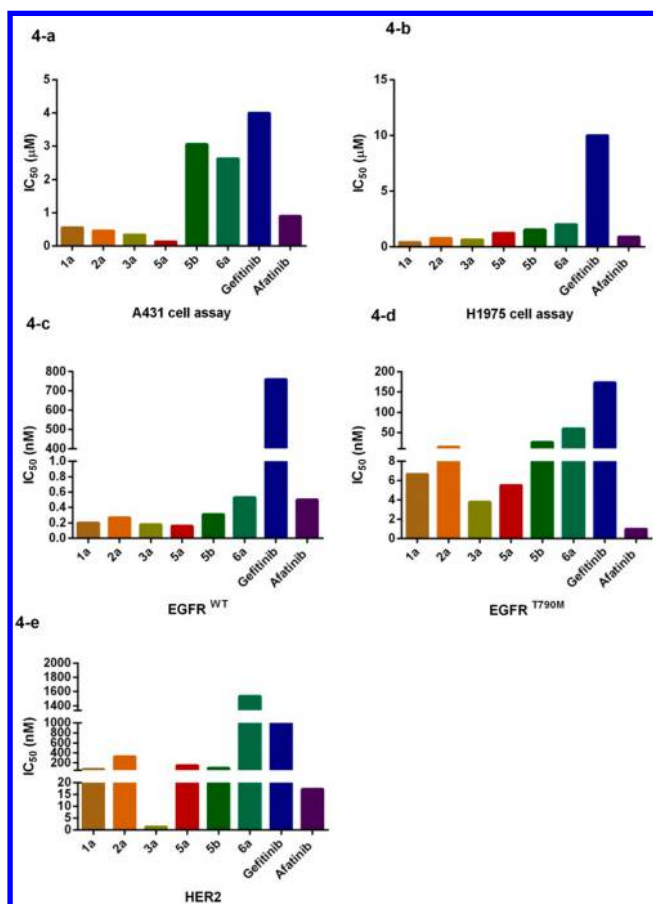
17.3 nM), with the exception of compound 3a (IC<sub>50</sub> = 1.38 nM). Activities of compounds 1–12 against tumor cells expressing EGFR mutations are demonstrated in two cancer cell lines (Table 1). Gefitinib-sensitive cell line A431 is an epidermoid cell that is driven by amplified wild-type EGFR. Gefitinib-resistant cell line NCI-H1975 harbors the EGFR<sup>L858R/T790M</sup> double mutation. The most enzymatically potent compounds, 1a, 3a, and 5a, also exhibit potent growth inhibitory activities in the A431 cells with IC<sub>50</sub> values of 0.55, 0.34, and 0.13  $\mu$ M, respectively, and are more potent than gefitinib. More importantly, compounds 1a, 3a, and 5a display high inhibitory activities against the growth of gefitinib-resistant H1975 cells, similar to the effects of afatinib. Together, six hit compounds were identified that retained similar *in vitro* potency to afatinib (Figure 3).

Table 1. In Vitro Antiproliferative Activities against Gefitinib-Sensitive and -Resistant Cell Lines and the EGFR-TK Inhibitory Activities of Compounds 1–12



Compd	R <sub>1</sub>	R <sub>2</sub>	R <sub>3</sub>	Anti-proliferation IC <sub>50</sub> (μM) <sup>a</sup>		Kinase Inhibition IC <sub>50</sub> (nM) <sup>b</sup>		
				A431	H1975	EGFR <sub>[WT]</sub>	EGFR <sup>T790M</sup>	HER2
1a(Z)		CH <sub>3</sub>		0.55	0.41	0.20	6.67	75.0
2a(Z)		CH <sub>3</sub>		0.46	0.76	0.27	14.5	324.4
2b(E)		CH <sub>3</sub>		0.68	1.01	0.67	-	-
3a(Z)		CH <sub>2</sub> CH <sub>2</sub>		0.34	0.64	0.18	3.77	1.38
3b(E)		CH <sub>2</sub> CH <sub>2</sub>		0.98	1.13	0.89	-	-
4a(Z)				11.5	4.37	0.26	21.3	1574
4b(E)				10.9	3.01	1.00	42.9	-
5a(Z)				0.13	1.24	0.16	5.52	149.4
5b(E)				3.06	1.53	0.31	25.8	97.1
6a(Z)		CH <sub>3</sub>		2.63	2.02	0.53	59.8	1536
6b(E)		CH <sub>3</sub>		0.83	1.11	0.30	-	-
7a(Z)				1.56	0.29	2.60	16.4	-
7b(E)				1.80	0.71	2.55	-	-
8a(Z)		CH <sub>2</sub> CH <sub>2</sub>		3.49	3.60	12.9	37.9	-
8b(E)		CH <sub>2</sub> CH <sub>2</sub>		24.8	6.42	39.2	-	-
9a(Z)		CH <sub>3</sub>		4.02	2.06	1.56	2.1	-
9b(E)		CH <sub>3</sub>		1.69	2.00	1.30	-	-
10a(Z)		CH <sub>2</sub> CH <sub>2</sub>		1.67	2.49	4.50	7.10	-
10b(E)		CH <sub>2</sub> CH <sub>2</sub>		5.90	2.94	9.50	-	-
11a(Z)		CH <sub>2</sub> CH <sub>2</sub>		0.75	1.19	3.60	3.50	-
11b(E)		CH <sub>2</sub> CH <sub>2</sub>		1.34	2.98	11.2	-	-
12a(Z)		CH <sub>3</sub>		2.10	3.30	2.60	8.30	-
12b(E)		CH <sub>3</sub>		1.20	4.10	5.00	-	-
	gefitinib			4.00	10.0	76.0	1730	1000
	afatinib			0.90	0.90	0.50	0.97	17.3

<sup>a</sup>The antiproliferative activities of the compounds were evaluated using the CellTiter-Glo (Promega) Kit assay. The data shown are the means from three independent experiments. <sup>b</sup>The kinase inhibitory activities of the compounds were evaluated using the Homogeneous time-resolved fluorescence (HTRF) method (Cisbio) assay. The data shown are the means from three independent experiments.



**Figure 3.** Antiproliferative activities and the kinase inhibitory activities of selected compounds.  $IC_{50}$  values for A431 (4-a), NSCLC H1975 cell (4-b), EGFR<sup>WT</sup> (4-c), EGFR<sup>T790M</sup> (4-d), and HER2 (4-e), treated with indicated drugs. Values were calculated from at least eight data points. In general three independent determinations were performed.

The specificity of one of the most potent compounds, **1a**, was profiled against a commercial panel of 16 kinases (Table 2). These kinases contain a cysteine residue that is sufficiently sensitive for electrophilic modification by many drugs, such as Akt1 (Cys296/Cys310), PDGFR $\alpha$  (Cys814), FGFR2 (Cys486), and Src (Cys345).<sup>24</sup> As shown in Table 2, compound **1a** demonstrates a favorable selectivity profile. EGFR<sup>WT</sup> and EGFR<sup>T790M</sup> are the only two kinases that experience marked inhibition ( $IC_{50}$  of 0.20 and 6.67 nM, respectively). These

**Table 2.** Selectivity Profiles for Compound **1a** versus a Panel of 16 Kinase Targets<sup>a</sup>

kinase	$IC_{50}$ (nM)	kinase	$IC_{50}$ (nM)
EGFR	0.20	AIK	>10000
EGFR <sup>T790M</sup>	6.67	AKT1	>10000
HER2	75.0	AKT2	>10000
HER4	23.0	c-Met	>10000
PDGFR $\alpha$	3596	FGFR2	>10000
PDGFR $\beta$	2102	FLT3	6810
JAK2	>10000	ABL	2262
SYK	>10000	SRC	1731

<sup>a</sup>The kinase inhibitory activities of the compounds were evaluated using the homogeneous time-resolved fluorescence (HTRF) method (Cisbio) assay. The data shown are the means from three independent experiments.

findings confirm that attenuated electrophiles conjugated to quinazolines would have a reduced likelihood of reacting with nonspecific proteins.

These promising enzymatic and cellular potencies promoted us to further investigate the pharmacokinetic profiles. The influence of geometric isomerism on the compound clearance ( $Cl_{int}$ ) induced in various microsomes demonstrated remarkable differences between *cis*- and *trans*- isomer pairs (Supporting Information, Table S1 and Table 3). The *cis*-

**Table 3.** Microsomal Stability and CYPs Inhibition Study of Selected Compounds

compd	$Cl_{int}$ ( $\mu$ L/min/mg protein)					$IC_{50}$ ( $\mu$ M) CYPs inhibition (3A4, 2D6, 2C9, 1A2, and 2C19)
	HLM	RLM	mouse LM	dog LM	monkey LM	
<b>1a</b>	14	18	45	194	128	>10
<b>2a</b>	37	11	31	34	102	>10
<b>3a</b>	27	33	47	95	97	>10
<b>5a</b>	2	14	12	39	31	>10
canertinib	50	105	5	26	221	
afatinib	8	12	6	9	24	

isomer analogues suffer a 5–10-fold reduction in human, rat, and mouse liver microsomal stability when compared to the corresponding *trans*-isomers. For instance, the  $Cl_{int}$  values for compounds **5a** and **5b** in human microsome were 2  $\mu$ L/min/mg protein and 60  $\mu$ L/min/mg protein, respectively. The same trend was observed for **2a/2b** (**2a**, 37  $\mu$ L/min/mg protein; **2b**, 151  $\mu$ L/min/mg protein), **4a/4b** (**4a**, 22  $\mu$ L/min/mg protein; **4b**, 124  $\mu$ L/min/mg protein) and **6a/6b** (**6a**, 18  $\mu$ L/min/mg protein; **6b**, 190  $\mu$ L/min/mg protein). Replacing the *N,N*-dimethyl group of compound **1a** with a polar piperidine obtained compound **2a** with an increasing dog LM stability (**1a**, 194  $\mu$ L/min/mg protein, vs **2a**, 34  $\mu$ L/min/mg protein). Modifying the 7-position of compound **1a** with (*S*)-tetrahydrofuran-3-ol led to compound **5a** with a remarkable increase in microsomal stability (HLM, RLM, mouse LM, dog LM, and monkey LM). These compounds were also evaluated for their ability to inhibit the major drug metabolizing enzymes. The inhibition of cytochrome P450 enzymes (CYPs) was evaluated by determining the activity of the compounds against CYPs 3A4, 2D6, 2C9, 1A2, and 2C19 in human liver microsomes. The results reveal essentially no inhibition, with  $IC_{50}$  values >10  $\mu$ M (Supporting Information, Table S2 and Table 3).

Selected *trans*-isomers were further evaluated for their great potency. The pharmacokinetic profiles in BALB/c mice are summarized in Supporting Information, Table S3, and Table 4.

Encouragingly, our studies demonstrated that the selected *trans*-isomers possessed greater oral bioavailability, higher maximal plasma concentration, and lower clearance rates than that of afatinib at an oral dose of 10 mg/kg. Also, the *cis*-isomer **2b** exhibited a reduced oral bioavailability ( $F = 16.5\%$ ) compared with its *trans*-isomer pair **2a**.

The concentration of selected compounds in various tissues was detected at multiple time points over 6 h following a 30 mg/kg oral dose in BALB/c mice (Table 4 and Supporting Information, Table S4–S7). The mean drug concentration of all tested compounds in the lung is 10–25-fold higher than in plasma. Additionally, the concentration in the brain is higher than that of afatinib, especially with compounds **2a** and **5a**. This

Table 4. Pharmacokinetic Properties of Selected Compounds in BALB/c Mice

compd	AUC(0–∞) (PO, $\mu\text{M}\cdot\text{min}$ )	$C_{\text{max}}$ (PO, $\mu\text{M}$ )	$\text{CL}_z$ (L/min/kg)	$V_z$ (L/kg)	$F$ (%)	lung/plasma/brain ratio <sup>c</sup>
1a <sup>a</sup>	460	0.79	0.05	14.0	98.5	nd <sup>d</sup>
2a <sup>b</sup>	306	0.83	0.04	7.14	105	20/1.0/2.31
2b <sup>b</sup>	14.7	0.09	0.12	12.2	16.5	nd <sup>d</sup>
3a <sup>a</sup>	994	2.66	0.02	3.94	89.4	11/1.0/0.29
5a <sup>a</sup>	625	0.94	0.03	9.69	84.7	25/1.0/0.79
afatinib <sup>a</sup>	29.4	0.13	0.27	36.2	37.4	18/1.0/0.14

<sup>a</sup>Compound 1a, 3a, 5a, and afatinib were administered PO to fed male BALB/c mice at a dose of 10 mg/kg. <sup>b</sup>Compound 2a and 2b were administered PO to fed male BALB/c mice at a dose of 5 mg/kg. <sup>c</sup>Compounds 2a, 3a, 5a, and afatinib were administered PO at a dose of 30 mg/kg. <sup>d</sup>Not detected.

indicates that the quinazoline analogues bearing fluoro-substituted olefins experience enhanced brain uptake thereby rendering them viable for the treatment of NSCLC patients with brain metastasis. Also, the hERG potassium channel patch clamp assay<sup>25</sup> shows that the selected compounds have an  $\text{IC}_{50} > 10 \mu\text{M}$ . These results indicate that these analogues have minimal potential for cardiac toxicity (Table 5).

Table 5. Inhibition of hERG Currents by Compounds 1a, 2a, 3a, 4a, 5a, and 5b

compd	no. of cells tested	% inhibition at 1 $\mu\text{M}$	% inhibition at 10 $\mu\text{M}$
1a	4	2.55 $\pm$ 3.92	18.4 $\pm$ 3.71
2a	4	0.71 $\pm$ 1.22	11.8 $\pm$ 5.98
3a	4	0 $\pm$ 0	3.06 $\pm$ 3.49
4a	4	0.94 $\pm$ 1.64	11.1 $\pm$ 2.34
5a	3	0 $\pm$ 0	14.8 $\pm$ 4.15
5b	4	6.37 $\pm$ 7.28	39.5 $\pm$ 4.76
cisapride	2	92.4 $\pm$ 3.47 at 1 $\mu\text{M}$ (65.5 $\pm$ 0.1 at 0.1 $\mu\text{M}$ )	

The cytotoxicity of compound 5a, afatinib, and doxorubicin against the colon cancer cell line SW620 was also evaluated. The colon cancer cell line SW620 expresses neither EGFR nor HER-2 to a significant extent and therefore is a good counterscreen cell line for EGFR-targeting inhibitors. As shown in Figure 4, compound 5a exhibited only an 11.5% growth inhibition of the cancer cell line SW620 at a concentration of 5  $\mu\text{M}$ . In contrast, at the concentration of 5  $\mu\text{M}$ , both afatinib and doxorubicin exhibited inhibition of 78.0% and 79.8%, respectively. These results indicate that compound 5a possesses less cytotoxicity against the EGFR-

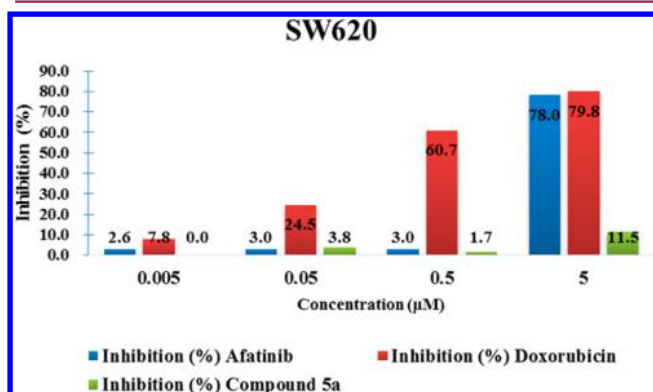


Figure 4. Cytotoxicity comparison of compound 5a and afatinib in EGFR-independent cancer cell line SW620.

independent cell line SW620 when compared to afatinib and doxorubicin.

Given the potent inhibition of EGFR<sup>T790M</sup> kinase and H1975 cell growth, together with the promising pharmacokinetic properties, the in vivo antitumor efficacy of compounds 2a, 3a, and 5a were evaluated using an EGFR<sup>L858R/T790M</sup>-driven human H1975 xenograft mouse model. The tumor growth values ( $T/C$  %) of compounds 2a, 3a, 5a, and afatinib were found to be 67.4%, 15.6%, 19.5%, and 30.3% at a dose of 30 mg/kg/day, respectively (Figure 5 and Supporting Information, Figure S1).

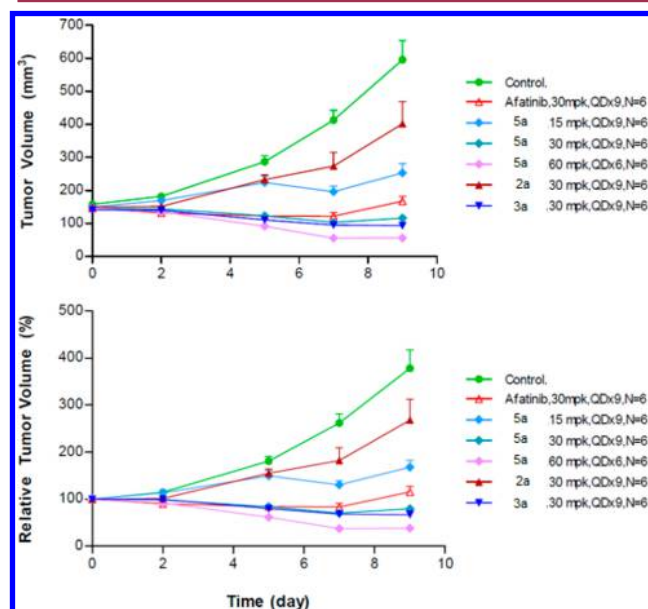


Figure 5. Effect on tumor volume in xenograft model of H1975 of compounds 2a, 3a, 5a, and afatinib. ( $T/C$  %) = mean RTV of the treated group/mean RTV of the control group  $\times$  100%. The individual relative tumor volume (RTV) was calculated as follows:  $\text{RTV} = V_t/V_0$ , where  $V_t$  is the volume on each day of measurement, and  $V_0$  is the volume on the day of initial treatment.

In addition, compound 5a displays dose-dependent inhibition of tumor growth. The  $T/C$  values are 42.5%, 19.5%, and 9.4% at dosages of 15, 30, and 60 mg/kg/day, respectively (Figure 5). Importantly, the compound 5a is well-tolerated, with no mortality or significant loss of body weight observed during treatment at a dose of 30 mg/kg.

## CONCLUSION

In this study, we report a new chemically tuned strategy to alter the overall biological profile of covalent EGFR inhibitors. The lead compound 5a exhibited potent inhibition of EGFR

mutation T790 M as well as gefitinib-resistant cell line H1975. Additionally, compound **5a** displayed weak inhibition against SW620, an EGFR-independent cell line. Further studies showed that compound **5a** possessed good pharmacokinetic profiles, favorable tissue distribution as well as an acceptable safety index. An in vivo antitumor efficacy study demonstrated that **5a** significantly inhibited tumor growth in an EGFR<sup>L858R/T790M</sup>-driven human NSCLC xenograft nude mouse model of H1975 at a dose of 30 mg/kg/day. The biological results demonstrate that compound **5a**, a quinazoline derivative bearing fluoro-substituted olefin tuned to alter Michael addition reactivity, is more potent and less toxic than afatinib. These findings provide the basis of a promising strategy toward the development of novel inhibitors with enhanced biological profiles.

## EXPERIMENTAL SECTION

**General Procedure.** Unless otherwise noted, all solvents and chemicals were used as purchased without further purification. <sup>1</sup>H NMR spectra were recorded on a Bruker DRX-500 [Bruker Biospin, Germany], Bruker AVANCE III-400, and Varian Mercury-300. Chemical shifts are reported in ppm relative to the residual solvent peak (CDCl<sub>3</sub>, TMS: 0.00). Multiplicity was indicated as follows: s (singlet); d (doublet); t (triplet); q (quartet); m (multiplet); dd (doublet of doublet); dt (triplet of doublet); td (doublet of triplet); brs (broad singlet), etc. Intermediates were purified by column chromatography on silica gel (200–300 mesh), and the separation of the *Z–E* isomers were performed on GILSON 215 semiprep HPLC using PhenomenexGimini 10 μm C18, 30 mm × 250 mm column at a flow rate of 30 mL/min or Thar SFC Pre80 (supercritical fluid chromatography, SFC) using an Agela AD-H 5 μm, 20 mm × 250 mm column at a flow rate of 50 g/min using gradients MeOH (containing 0.1% DEA): CO<sub>2</sub> = 40:60. All reported yields are isolated yields after column chromatography. Purity of all biologically evaluated compounds was determined by HPLC analysis to be >95%. HPLC analysis was performed on Agilent 1200 using Agilent Eclipse XDB-C18 5 μm 4.6 mm × 150 mm at a flow rate of 1 mL/min using the listed gradients: (mobile phase A, MeOH; mobile phase B, MeCN; mobile phase C, 0.01 mol/L KH<sub>2</sub>PO<sub>4</sub>, pH = 3.0) (Table 6).

**Table 6**

t/min	mobile phase A (%)	mobile phase B (%)	mobile phase C (%)
0	5	0	95
1.6	5	0	95
8.5	10	20	70
13	10	20	70
18	15	35	50
30	15	50	35
35	15	50	35
36.5	5	0	95
40	5	0	95

The HPLC-HRMS of all compounds was confirmed on a Agilent 1290 HPLC-6224 time-of-flight mass spectrometer using PhenomenexLuna 5 μm C18, 100 Å, 150 mm × 4.6 mm 5 μm column at a flow rate of 0.5 mL/min using liner gradients buffer B in A (B, CH<sub>3</sub>OH containing 0.1% formic acid; A, H<sub>2</sub>O containing 0.1% formic acid). Mobile phase B was increased linearly from 5% to 95% over 7 min and 95% over the next 2 min, after which the column was equilibrated to 5% for 1 min.

**2-(Diethoxyphosphoryl)-2-fluoroacetic Acid (II).** To a solution of 2-(diethoxyphosphinyl)-2-fluoroacetic acid ethyl ester (4.5 g, 18.6 mmol) in 180 mL of ethanol was added a solution of sodium hydroxide (3.72 g, 93 mmol) in water (180 mL). The reaction mixture was stirred for 2 h at –5 °C and acidified to pH = 2–3 with 4 N HCl.

The reaction mixture was evaporated under reduced pressure at room temperature to give the crude product, and the crude was dissolved in acetone to precipitate the salt, filtered, and the filtrate evaporated under reduced pressure to give the corresponding acid as white waxy solid; yield 95% (3.78 g). <sup>1</sup>H NMR (500 MHz, CDCl<sub>3</sub>) δ 5.27 (dd, *J* = 47.0, 13.0 Hz, 1H), 4.36–4.26 (m, 4H), 1.42–1.36 (m, 6H). HRMS (ESI): *m/z* calcd for (C<sub>6</sub>H<sub>12</sub>FO<sub>3</sub>P + H)<sup>+</sup>, 215.0484; found, 215.0494.

**(S)-N<sup>4</sup>-(3-Chloro-4-fluorophenyl)-7-((tetrahydrofuran-3-yl)oxy)quinazoline-4,6-diamine (III-a).** To a solution of (S)-4-(3-chloro-4-fluorophenyl)-7-((tetrahydrofuran-3-yl)oxy)-6-nitro-quinazoline (2.02 g, 5.0 mmol) and NiCl<sub>2</sub>·6H<sub>2</sub>O (2.38 g, 10 mmol) in 40 mL of MeOH/DCM (V/V = 1:4) was added NaBH<sub>4</sub> (0.76 g, 20 mmol) at 0 °C. The mixture was stirred at 0 °C for 30 min then at room temperature for 30 min. The mixture was filtered, and the filtrate was evaporated to dryness under reduce pressure. The crude product was purified by flash column chromatography on silica gel eluting with CH<sub>2</sub>Cl<sub>2</sub>/MeOH = 10:1; yellow solid; yield 90% (1.68 g). <sup>1</sup>H NMR (500 MHz, DMSO) δ 10.26 (s, 1H), 8.56 (s, 1H), 8.11 (s, 1H), 7.76 (s, 1H), 7.57 (s, 1H), 7.46 (t, *J* = 9.0 Hz, 1H), 7.24 (s, 1H), 5.70 (s, 2H), 5.22 (s, 1H), 4.02–3.99 (m, 2H), 3.95–3.91 (m, 1H), 3.81–3.80 (m, 1H), 2.36–2.32 (m, 1H), 2.15–2.13 (m, 1H). HRMS (ESI): *m/z* calcd for (C<sub>18</sub>H<sub>16</sub>ClFN<sub>4</sub>O<sub>2</sub> + H)<sup>+</sup>, 375.1024; found, 375.1012.

**Diethyl (2-((4-((3-Chloro-4-fluorophenyl)amino)-7-((S)-tetrahydrofuran-3-yl)oxy)quinazolin-6-yl)amino)-1-fluoro-2-oxoethyl)phosphonate (IV-a).** To a solution of the above compound (III-a) (0.37 g, 1.0 mmol) and Et<sub>3</sub>N (0.15 g, 1.5 mmol) in DMF (10 mL) was added dropwise a solution of compound (II) (0.32 g, 1.5 mmol) in DMF (5 mL) at ice bath. The reaction mixture was stirred at ice bath for 30 min and then warmed to room temperature for overnight. The completion of the reaction was detected via LC-MS. After completion, the reaction was quenched with saturated aqueous NaHCO<sub>3</sub> and then extracted with EtOAc (30 mL × 3) three times. The organic layer was dried over anhydrous Na<sub>2</sub>SO<sub>4</sub> and evaporated under reduced pressure. The crude product was purified by silica gel with DCM/MeOH = 40:1; yellow solid; yield 60% (0.34 g). <sup>1</sup>H NMR (500 MHz, DMSO) δ 9.94 (s, 1H), 9.64 (s, 1H), 8.89 (s, 1H), 8.55 (s, 1H), 8.09 (dd, *J* = 6.5, 2.5 Hz, 1H), 7.78–7.75 (m, 1H), 7.43 (t, *J* = 9.0 Hz, 1H), 7.34 (s, 1H), 6.02 (dd, *J* = 45.0, 11.0 Hz, 1H), 5.22 (s, 1H), 4.20 (dd, *J* = 15.0, 7.0 Hz, 4H), 4.02–3.99 (m, 2H), 3.95–3.91 (m, 1H), 3.81–3.80 (m, 1H), 2.36–2.32 (m, 1H), 2.15–2.13 (m, 1H), 1.29 (dt, *J* = 10.0, 7.0 Hz, 6H). HRMS (ESI): *m/z* calcd for (C<sub>24</sub>H<sub>26</sub>ClF<sub>2</sub>N<sub>4</sub>O<sub>6</sub>P + H)<sup>+</sup>, 571.1325; found, 571.1335.

**Diethyl (2-((4-((3-Chloro-4-fluorophenyl)amino)-7-methoxyquinazolin-6-yl)amino)-1-fluoro-2-oxoethyl)phosphonate (VI-b).** The preparation was according to the compound (VI-a). The crude product was purified by silica gel with DCM/MeOH = 40:1; yellow solid; yield 70% (0.36 g). <sup>1</sup>H NMR (500 MHz, DMSO) δ 9.94 (s, 1H), 9.64 (s, 1H), 8.89 (s, 1H), 8.55 (s, 1H), 8.09 (dd, *J* = 6.5, 2.5 Hz, 1H), 7.77 (ddd, *J* = 9.0, 4.0, 2.5 Hz, 1H), 7.43 (t, *J* = 9.0 Hz, 1H), 7.34 (s, 1H), 6.02 (dd, *J* = 45.0, 11.0 Hz, 1H), 4.20 (dd, *J* = 15.5, 8.0 Hz, 4H), 4.03 (s, 3H), 1.29 (dt, *J* = 10.0, 7.5 Hz, 6H).

**Diethyl (2-((4-((3-Chloro-4-(pyridin-2-ylmethoxy)phenyl)amino)-7-ethoxyquinazolin-6-yl)amino)-1-fluoro-2-oxoethyl)phosphonate (VI-c).** The preparation was according to the compound (VI-a). The crude product was purified by silica gel with DCM/MeOH = 40:1; yellow solid; yield 50% (0.31 g). <sup>1</sup>H NMR (500 MHz, DMSO) δ 9.81 (s, 1H), 9.49 (s, 1H), 8.87 (s, 1H), 8.60 (d, *J* = 4.0 Hz, 1H), 8.49 (s, 1H), 7.94 (d, *J* = 2.0 Hz, 1H), 7.89 (td, *J* = 8.0, 2.0 Hz, 1H), 7.65 (dd, *J* = 9.0, 2.5 Hz, 1H), 7.59 (d, *J* = 8.0 Hz, 1H), 7.40–7.35 (m, 1H), 7.29 (s, 1H), 7.25 (d, *J* = 9.0 Hz, 1H), 6.03 (dd, *J* = 45.0, 11.5 Hz, 1H), 5.29 (s, 2H), 4.30 (q, *J* = 7.0 Hz, 2H), 4.26–4.14 (m, 4H), 1.44 (t, *J* = 7.0 Hz, 3H), 1.29 (dt, *J* = 13.5, 7.0 Hz, 6H).

**Diethyl (2-((4-((3-Chloro-4-((3-fluorobenzyl)oxy)phenyl)amino)-7-methoxyquinazolin-6-yl)amino)-1-fluoro-2-oxoethyl)phosphonate (VI-d).** The preparation was according to the compound (VI-a). The crude product was purified by silica gel with DCM/MeOH = 40:1; yellow solid; yield 50% (0.31 g). <sup>1</sup>H NMR (500 MHz, DMSO) δ 9.84 (s, 1H), 9.66 (s, 1H), 8.86 (s, 1H), 8.50 (s, 1H), 7.94 (s, 1H), 7.67–7.65 (m, 1H), 7.48–7.46 (m, 1H), 7.34–7.31 (m, 3H), 7.25 (d, *J* = 9.0 Hz, 2H), 7.21–7.18 (m, 1H), 6.03 (dd, *J* = 45.0, 11.0

Hz, 1H), 5.26 (s, 2H), 4.20 (dd,  $J = 14.0, 7.0$  Hz, 4H), 4.02 (s, 3H), 1.29 (dd,  $J = 14.0, 7.0$  Hz, 6H).

**Diethyl 2-((4-((3-Bromophenyl)amino)-7-methoxyquinazolin-6-yl)amino)-1-fluoro-2-oxoethyl)phosphonate (VI-e).** The preparation was according to the compound (VI-a). The crude product was purified by silica gel with DCM/MeOH = 40:1; yellow solid; yield 75% (0.41 g).  $^1\text{H NMR}$  (500 MHz, DMSO)  $\delta$  9.94 (s, 1H), 9.67 (s, 1H), 8.90 (s, 1H), 8.57 (s, 1H), 8.13 (s, 1H), 7.83 (d,  $J = 8.5$  Hz, 1H), 7.37–7.32 (m, 2H), 7.29 (d,  $J = 8.0$  Hz, 1H), 6.03 (dd,  $J = 45.0, 11.0$  Hz, 1H), 4.21 (dd,  $J = 15.0, 7.5$  Hz, 4H), 4.03 (s, 3H), 1.29 (dt,  $J = 9.5, 7.0$  Hz, 6H).

**1-(2,2-Dimethoxyethyl)piperidine (VII-a).** A mixture of 2-bromoacetaldehyde diethyl acetal (4.18 g, 25 mmol), piperidine (2.13 g, 25 mmol), and  $\text{K}_2\text{CO}_3$  (6.9 g, 50 mmol) was stirred at 120 °C for 16 h. The reaction was cooled to room temperature, diluted with water (20 mL), and extracted with DCM (3 × 30 mL) three times. The combined organic layer was washed with saturated aqueous  $\text{NaHCO}_3$  and brine, dried over anhydrous  $\text{Na}_2\text{SO}_4$ , filtered, and concentrated to get colorless oil directly for further reaction. HRMS (ESI):  $m/z$  calcd for ( $\text{C}_9\text{H}_{19}\text{NO}_2 + \text{H}$ ) $^+$ , 174.1494; found, 174.1498.

**2-(Piperidin-1-yl)acetaldehyde Hydrochloride (VIII-a).** A solution of intermediate (VII-a) (1.73 g, 10 mmol) dissolved in concentrated aqueous HCl (20 mL) was refluxed at 110 °C for 4.5 h. The reaction mixture was concentrated in reduced pressure to obtain dark oil, which was used without purification. HRMS (ESI):  $m/z$  calcd for ( $\text{C}_7\text{H}_{13}\text{NO} + \text{H}$ ) $^+$ , 128.1920; found, 128.1930.

***N*-4-((3-Chloro-4-fluorophenyl)amino)-7-methoxyquinazolin-6-yl)-4-(dimethylamino)-2-fluorobut-2-enamide (1a+1b).** NaOH (0.32 g, 8.0 mmol) was dissolved in EtOH– $\text{H}_2\text{O}$  (10 mL:1 mL). The phosphonate (0.24 g, 1.0 mmol) was added to the above solution. After the mixture became clear, the corresponding aldehyde (2.0 mmol) was added at 0–5 °C in an ice bath. The reaction mixture was warmed to room temperature and stirred at room temperature for the indicated time. The reaction mixture was adjusted to pH = 1–2 with 2 N HCl and washed with EtOAc (3 × 30 mL) three times. The aqueous layers were adjusted to pH = 10.0 with 4N NaOH and extracted with EtOAc (3 × 30 mL) three times. The combined organic layer was washed with brine, dried over anhydrous  $\text{Na}_2\text{SO}_4$ , and concentrated in reduced pressure to obtain the crude product. TLC  $R_f$  = 0.30 (EtOAc/MeOH = 5:1). The two isomers were not separated on the TLC plate. The separation of the *Z*–*E* isomers were performed on GILSON 215 semiprep HPLC using PhenomenexGimini 10  $\mu$  C18, 30 mm × 250 mm column at a flow rate of 30 mL/min using linear gradients mobile phase B in A (B,  $\text{CH}_3\text{CN}$  containing 0.05% ammonium hydroxide; A,  $\text{H}_2\text{O}$ ). Mobile phase B was increased linearly from 51% to 100% over 15.5 min and 100% over the next 2.5 min, after which the column was equilibrated to 51% for 2 min.

***Z*-N-4-((3-Chloro-4-fluorophenyl)amino)-7-methoxyquinazolin-6-yl)-4-(dimethylamino)-2-fluorobut-2-enamide (1a).** The retention time of *Z*-isomer is 14.5 min; light-yellow solid; yield 15%.  $^1\text{H NMR}$  (300 MHz, DMSO)  $\delta$  11.41 (s, 1H), 10.30 (s, 1H), 8.99 (s, 1H), 8.88 (s, 1H), 8.04 (dd,  $J = 2.7$  Hz, 1H), 7.77–7.70 (m, 1H), 7.58 (s, 1H), 7.56 (dd,  $J = 2.7$  Hz, 1H), 6.47 (td,  $J = 33.6, 7.5$  Hz, 1H), 4.03 (s, 3H), 3.99 (br, 2H), 2.79 (s, 6H).

***N*-4-((3-Chloro-4-fluorophenyl)amino)-7-methoxyquinazolin-6-yl)-2-fluoro-4-(piperidin-1-yl)but-2-enamide (2a+2b).** The preparation was according to the compound (1a+1b). TLC  $R_f$  = 0.53, 0.56 (DCM/MeOH = 10:1, the two isomers can be separated). The separation of the *Z*–*E* isomers were performed on Thar SFC Pre80 (supercritical fluid chromatography, SFC) using Agela AD-H 5  $\mu$ , 20 mm × 250 mm column at a flow rate of 50 g/min using gradients MeOH (containing 0.1% DEA):  $\text{CO}_2 = 40:60$ .

***Z*-N-4-((3-Chloro-4-fluorophenyl)amino)-7-methoxyquinazolin-6-yl)-2-fluoro-4-(piperidin-1-yl)but-2-enamide (2a).** The retention time of the *Z*-isomer is 6.85 min; light-yellow solid; yield 35.4%.  $^1\text{H NMR}$  (400 MHz,  $\text{CDCl}_3$ )  $\delta$  9.01 (s, 1H), 8.88 (d,  $J = 4.4$  Hz, 1H), 8.66 (s, 1H), 7.95 (dd,  $J = 6.8, 2.8$  Hz, 1H), 7.81 (dd,  $J = 3.2, 0.5$  Hz, 1H), 7.55 (ddd,  $J = 9.0, 4.0, 2.8$  Hz, 1H), 7.27 (s, 1H), 7.14 (t,  $J = 8.8$  Hz, 1H), 6.45 (dt,  $J = 36.0, 7.2$  Hz, 1H), 4.07 (s, 3H), 3.34 (d,  $J = 7.2$  Hz, 2H), 2.54–2.50 (m, 4H), 1.68–1.64 (m, 4H), 1.50–1.46 (m, 2H).

HRMS (ESI):  $m/z$  calcd for ( $\text{C}_{24}\text{H}_{24}\text{ClF}_2\text{N}_5\text{O}_2 + \text{H}$ ) $^+$ , 488.1665; found, 488.1656.

***E*-N-4-((3-Chloro-4-fluorophenyl)amino)-7-methoxyquinazolin-6-yl)-2-fluoro-4-(piperidin-1-yl)but-2-enamide (2b).** The retention time of the *E*-isomer is 4.65 min; light-yellow solid; yield 28.2%.  $^1\text{H NMR}$  (400 MHz,  $\text{CDCl}_3$ )  $\delta$  9.23 (s, 1H), 8.96 (s, 1H), 8.67 (s, 1H), 7.93 (dd,  $J = 6.8, 2.8$  Hz, 1H), 7.73 (s, 1H), 7.57 (ddd,  $J = 9.0, 4.0, 2.8$  Hz, 1H), 7.28 (s, 1H), 7.16 (t,  $J = 8.8$  Hz, 1H), 6.20 (dt,  $J = 22.8, 5.6$  Hz, 1H), 4.07 (s, 3H), 3.79–3.74 (m, 2H), 2.64–2.61 (m, 4H), 1.73–1.68 (m, 4H), 1.54–1.47 (m, 2H). HRMS (ESI):  $m/z$  calcd for ( $\text{C}_{24}\text{H}_{24}\text{ClF}_2\text{N}_5\text{O}_2 + \text{H}$ ) $^+$ , 488.1665; found, 488.1656.

***N*-4-((3-Chloro-4-(pyridin-2-ylmethoxy)phenyl)amino)-7-ethoxyquinazolin-6-yl)-4-(dimethylamino)-2-fluorobut-2-enamide (3a+3b).** The preparation was according to the compound (1a+1b). TLC  $R_f$  = 0.53, 0.56 (DCM/MeOH = 10:1, the two isomers could be separated). The separation of the *Z*–*E* isomers was performed according to compound (2a+2b).

***Z*-N-4-((3-Chloro-4-(pyridin-2-ylmethoxy)phenyl)amino)-7-ethoxyquinazolin-6-yl)-4-(dimethylamino)-2-fluorobut-2-enamide (3a).** The retention time of *Z*-isomer is 5.12 min; light-yellow solid; yield 34.2%.  $^1\text{H NMR}$  (400 MHz,  $\text{CDCl}_3$ )  $\delta$  9.00 (s, 1H), 8.98 (d,  $J = 5.6$  Hz, 1H), 8.63 (s, 1H), 8.59 (d,  $J = 4.4$  Hz, 1H), 7.88 (d,  $J = 2.8$  Hz, 1H), 7.79–7.78 (m, 1H), 7.75 (d,  $J = 7.6, 1.6$  Hz, 1H), 7.67 (d,  $J = 8.0$  Hz, 1H), 7.52 (dd,  $J = 8.8, 2.8$  Hz, 1H), 7.25 (s, 1H), 7.01 (d,  $J = 8.8$  Hz, 1H), 6.39 (dt,  $J = 36.4, 7.2$  Hz, 1H), 5.30 (s, 2H), 4.30 (q,  $J = 6.8$  Hz, 2H), 3.26 (dd,  $J = 7.2, 2.4$  Hz, 2H), 2.32 (s, 6H), 1.57 (t,  $J = 7.2$  Hz, 4H). HRMS (ESI):  $m/z$  calcd for ( $\text{C}_{28}\text{H}_{28}\text{ClFN}_6\text{O}_3 + \text{H}$ ) $^+$ , 551.1973; found, 551.1967.

***E*-N-4-((3-Chloro-4-(pyridin-2-ylmethoxy)phenyl)amino)-7-ethoxyquinazolin-6-yl)-4-(dimethylamino)-2-fluorobut-2-enamide (3b).** The retention time of the *E*-isomer is 6.06 min; light-yellow solid; yield 25.8%.  $^1\text{H NMR}$  (400 MHz,  $\text{CDCl}_3$ )  $\delta$  9.19 (d,  $J = 4.8$  Hz, 1H), 8.98 (s, 1H), 8.65 (s, 1H), 8.60 (dd,  $J = 5.6, 0.8$  Hz, 1H), 7.86 (d,  $J = 2.8$  Hz, 1H), 7.78–7.74 (m, 1H), 7.7–7.66 (m, 1H), 7.55–7.52 (m, 1H), 7.48–7.47 (m, 1H), 7.03 (d,  $J = 9.2$  Hz, 1H), 6.25–6.19 (m, 1H), 5.35 (m, 1H), 5.30 (s, 2H), 4.31 (q,  $J = 7.2$  Hz, 2H), 3.96–3.92 (m, 2H), 2.59–2.55 (s, 6H), 1.57 (t,  $J = 6.8$  Hz, 3H). HRMS (ESI):  $m/z$  calcd for ( $\text{C}_{28}\text{H}_{28}\text{ClFN}_6\text{O}_3 + \text{H}$ ) $^+$ , 551.1973; found, 551.1969.

***S*-N-4-((3-Chloro-4-fluorophenyl)amino)-7-((tetrahydrofuran-3-yl)oxy)quinazolin-6-yl)-2-fluoro-4-morpholinobut-2-enamide (4a+4b).** The preparation was according to the compound (1a+1b). TLC  $R_f$  = 0.52, 0.56 (DCM/MeOH = 10:1, the two isomers could be separated). The separation of the *Z*–*E* isomers was performed according to compound (2a+2b).

***Z*-N-4-((3-Chloro-4-fluorophenyl)amino)-7-((tetrahydrofuran-3-yl)oxy)quinazolin-6-yl)-2-fluoro-4-morpholinobut-2-enamide (4a).** The retention time of the *Z*-isomer is 5.52 min; light-yellow solid; yield 24.0%.  $^1\text{H NMR}$  (400 MHz,  $\text{CDCl}_3$ )  $\delta$  9.03 (s, 1H), 8.91 (d,  $J = 4.4$  Hz, 1H), 8.67 (s, 1H), 7.97 (dd,  $J = 6.4, 2.4$  Hz, 1H), 7.75 (s, 1H), 7.59–7.55 (m, 1H), 7.22 (s, 1H), 7.17 (t,  $J = 8.8$  Hz, 1H), 6.40 (dt,  $J = 36.4, 6.4$  Hz, 1H), 5.21 (s, 2H), 4.14–4.05 (m, 4H), 4.00–3.94 (m, 1H), 3.76–3.74 (m, 4H), 3.31 (dd,  $J = 7.2, 2.4$  Hz, 2H), 2.55–2.53 (m, 4H). HRMS (ESI):  $m/z$  calcd for ( $\text{C}_{26}\text{H}_{26}\text{ClF}_2\text{N}_5\text{O}_4 + \text{H}$ ) $^+$ , 546.1719; found, 546.1706.

***E*-N-4-((3-Chloro-4-fluorophenyl)amino)-7-((tetrahydrofuran-3-yl)oxy)quinazolin-6-yl)-2-fluoro-4-morpholinobut-2-enamide (4b).** The retention time of the *E*-isomer is 3.11 min; light-yellow solid; yield 17.4%.  $^1\text{H NMR}$  (400 MHz,  $\text{CDCl}_3$ )  $\delta$  9.02 (s, 1H), 8.98 (d,  $J = 6.0$  Hz, 1H), 8.67 (s, 1H), 7.96 (dd,  $J = 6.4, 2.8$  Hz, 1H), 7.59–7.55 (m, 2H), 7.22 (s, 1H), 7.19 (d,  $J = 8.8$  Hz, 1H), 6.08 (dt,  $J = 23.6, 6.4$  Hz, 1H), 5.20 (s, 2H), 4.10–4.04 (m, 4H), 4.00–3.96 (m, 1H), 3.76–3.74 (m, 4H), 3.71 (dd,  $J = 6.8, 2.4$  Hz, 2H), 2.58–2.55 (m, 4H). HRMS (ESI):  $m/z$  calcd for ( $\text{C}_{26}\text{H}_{26}\text{ClF}_2\text{N}_5\text{O}_4 + \text{H}$ ) $^+$ , 546.1719; found, 546.1706.

***S*-N-4-((3-Chloro-4-fluorophenyl)amino)-7-((tetrahydrofuran-3-yl)oxy)quinazolin-6-yl)-4-(dimethylamino)-2-fluorobut-2-enamide (5a+5b).** The preparation was according to the compound (1a+1b). TLC  $R_f$  = 0.53, 0.58 (DCM/MeOH = 10:1, the two isomers could be separated). The separation of the *Z*–*E* isomers was performed according to compound (2a+2b).

(Z)-(S)-N-(4-((3-Chloro-4-fluorophenyl)amino)-7-((tetrahydrofuran-3-yl)oxy)quinazolin-6-yl)-4-(dimethylamino)-2-fluorobut-2-enamide (**5a**). The retention time of the Z-isomer is 5.20 min; light-yellow solid; yield 45.5%. <sup>1</sup>H NMR (400 MHz, CDCl<sub>3</sub>) δ 9.05 (s, 1H), 8.91 (d, J = 6.8 Hz, 1H), 8.67 (s, 1H), 7.98 (dd, J = 6.8, 2.8 Hz, 1H), 7.73 (s, 1H), 7.59–7.55 (m, 1H), 7.22 (s, 1H), 7.18 (t, J = 8.8 Hz, 1H), 6.40 (dt, J = 36.4, 7.2 Hz, 1H), 5.22–5.19 (m, 1H), 4.12–4.07 (m, 4H), 4.00–3.94 (m, 1H), 3.26 (dd, J = 7.6, 2.8 Hz, 2H), 2.33 (s, 6H). HRMS (ESI): *m/z* calcd for (C<sub>24</sub>H<sub>24</sub>ClF<sub>2</sub>N<sub>5</sub>O<sub>3</sub> + H)<sup>+</sup>, 504.1614; found, 504.1605.

(E)-(S)-N-(4-((3-Chloro-4-fluorophenyl)amino)-7-((tetrahydrofuran-3-yl)oxy)quinazolin-6-yl)-4-(dimethylamino)-2-fluorobut-2-enamide (**5b**). The retention time of the E-isomer is 4.53 min; light-yellow solid; yield 24.5%. <sup>1</sup>H NMR (400 MHz, CDCl<sub>3</sub>) δ 9.26 (brs, 1H), 9.00 (s, 1H), 8.67 (s, 1H), 7.95 (dd, J = 6.4, 2.8 Hz, 1H), 7.62 (s, 1H), 7.59–7.54 (m, 1H), 7.22 (s, 1H), 7.18 (t, J = 8.8 Hz, 1H), 6.09 (dt, J = 24.8, 6.8 Hz, 1H), 5.20–5.16 (m, 2H), 4.10–4.04 (m, 4H), 3.98–3.95 (m, 1H), 3.60 (dd, J = 7.2, 2.8 Hz, 2H), 2.34 (s, 6H). HRMS (ESI): *m/z* calcd for (C<sub>24</sub>H<sub>24</sub>ClF<sub>2</sub>N<sub>5</sub>O<sub>3</sub> + H)<sup>+</sup>, 504.1614; found, 504.1603.

N-(4-((3-Chloro-4-fluorophenyl) amino)-7-methoxyquinazolin-6-yl)-2-fluoro-4-(piperidin-1-yl)but-2-enamide (**6a+6b**). The preparation was according to the compound (**1a+1b**). TLC R<sub>f</sub> = 0.52, 0.60 (DCM/MeOH = 10:1, the two isomers could be separated). The separation of the Z–E isomers was performed according to compound (**2a+2b**).

(Z)-N-(4-((3-Chloro-4-fluorophenyl)amino)-7-methoxyquinazolin-6-yl)-2-fluoro-4-(piperidin-1-yl)but-2-enamide (**6a**). The retention time of the Z-isomer is 3.82 min; light-yellow solid; yield 27.0%. <sup>1</sup>H NMR (400 MHz, CDCl<sub>3</sub>) δ 9.01 (s, 1H), 8.91 (d, J = 4.8 Hz, 1H), 8.67 (s, 1H), 7.95 (dd, J = 6.4, 2.4 Hz, 1H), 7.75 (s, 1H), 7.57–7.54 (m, 1H), 7.29 (s, 1H), 7.15 (t, J = 8.8 Hz, 1H), 6.38 (dt, J = 36.0, 7.2 Hz, 1H), 4.08 (s, 3H), 3.75 (t, J = 4.4 Hz, 4H), 3.31 (dd, J = 7.2, 2.4 Hz, 2H), 2.54 (t, J = 4.4 Hz, 4H). HRMS (ESI): *m/z* calcd for (C<sub>23</sub>H<sub>22</sub>ClF<sub>2</sub>N<sub>5</sub>O<sub>3</sub> + H)<sup>+</sup>, 490.1457; found, 490.1447.

(E)-N-(4-((3-Chloro-4-fluorophenyl) amino)-7-methoxyquinazolin-6-yl)-2-fluoro-4-(piperidin-1-yl)but-2-enamide (**6b**). The retention time of the E-isomer is 2.67 min; light-yellow solid; yield 18.6%. <sup>1</sup>H NMR (400 MHz, CDCl<sub>3</sub>) δ 9.05 (d, J = 5.2 Hz, 1H), 9.00 (s, 1H), 8.68 (s, 1H), 7.95 (dd, J = 6.4, 2.8 Hz, 1H), 7.58–7.54 (m, 2H), 7.30 (s, 1H), 7.17 (t, J = 8.4 Hz, 1H), 6.07 (dt, J = 23.6, 6.8 Hz, 1H), 4.08 (s, 3H), 3.75 (t, J = 4.8 Hz, 4H), 3.70 (dd, J = 6.8, 2.4 Hz, 2H), 2.57 (t, J = 4.8 Hz, 4H). HRMS (ESI): *m/z* calcd for (C<sub>23</sub>H<sub>22</sub>ClF<sub>2</sub>N<sub>5</sub>O<sub>3</sub> + H)<sup>+</sup>, 490.1457; found, 490.1451.

(S)-N-(4-((3-Chloro-4-fluorophenyl)amino)-7-((tetrahydrofuran-3-yl)oxy)quinazolin-6-yl)-2-fluoro-4-(piperidin-1-yl)but-2-enamide (**7a+7b**). The preparation was according to the compound (**1a+1b**). TLC R<sub>f</sub> = 0.52, 0.53 (DCM/MeOH = 10:1, the two isomers could be separated). The separation of the Z–E isomers was performed according to compound (**2a+2b**).

(Z)-(S)-N-(4-((3-Chloro-4-fluorophenyl)amino)-7-((tetrahydrofuran-3-yl)oxy)quinazolin-6-yl)-2-fluoro-4-(piperidin-1-yl)but-2-enamide (**7a**). The retention time of the Z-isomer is 13.05 min; light-yellow solid; yield 38.1%. <sup>1</sup>H NMR (400 MHz, DMSO) δ 9.84 (s, 1H), 9.64 (s, 1H), 8.75 (s, 1H), 8.57 (s, 1H), 8.15 (dd, J = 6.4, 2.0 Hz, 1H), 7.82–7.79 (m, 1H), 7.44 (t, J = 9.2 Hz, 1H), 7.31 (s, 1H), 6.20 (dt, J = 36.8, 6.8 Hz, 1H), 5.33 (t, J = 5.6 Hz, 1H), 3.99 (dd, J = 10.4, 4.4 Hz, 1H), 3.88 (d, J = 8.8 Hz, 2H), 3.82–3.77 (m, 1H), 3.19 (d, J = 6.0 Hz, 2H), 2.38–2.30 (m, 4H), 2.07–1.96 (m, 2H), 1.53–1.49 (m, 4H), 1.40–1.39 (m, 2H). HRMS (ESI): *m/z* calcd for (C<sub>27</sub>H<sub>28</sub>ClF<sub>2</sub>N<sub>5</sub>O<sub>3</sub> + H)<sup>+</sup>, 544.1927; found, 544.1914.

(E)-(S)-N-(4-((3-Chloro-4-fluorophenyl)amino)-7-((tetrahydrofuran-3-yl)oxy)quinazolin-6-yl)-2-fluoro-4-(piperidin-1-yl)but-2-enamide (**7b**). The retention time of the E-isomer is 11.19 min; light-yellow solid; yield 17.5%. <sup>1</sup>H NMR (400 MHz, DMSO) δ 10.06 (s, 1H), 9.84 (s, 1H), 8.74 (s, 1H), 8.57 (s, 1H), 8.14 (dd, J = 6.8, 2.4 Hz, 1H), 7.82–7.79 (m, 1H), 7.44 (t, J = 9.2 Hz, 1H), 7.32 (s, 1H), 6.09 (dt, J = 23.6, 13.6 Hz, 1H), 5.34 (t, J = 5.6 Hz, 1H), 4.00–3.97 (m, 1H), 3.90–3.85 (m, 2H), 3.82–3.79 (m, 1H), 3.47 (m, 2H), 2.41–2.33 (m, 4H), 2.07–1.96 (m, 2H), 1.51–1.48 (m, 4H), 1.39–1.37 (m, 2H).

HRMS (ESI): *m/z* calcd for (C<sub>27</sub>H<sub>28</sub>ClF<sub>2</sub>N<sub>5</sub>O<sub>3</sub> + H)<sup>+</sup>, 544.1927; found, 544.1914.

N-(4-((3-Chloro-4-((6-methylpyridin-3-yl)oxy)phenyl)amino)-7-ethoxyquinazolin-6-yl)-2-fluoro-4-(piperidin-1-yl)but-2-enamide (**8a+8b**). The preparation was according to the compound (**1a+1b**). TLC R<sub>f</sub> = 0.52, 0.54 (DCM/MeOH = 10:1, the two isomers could be separated). The separation of the Z–E isomers was performed according to compound (**2a+2b**).

(Z)-N-(4-((3-Chloro-4-((6-methylpyridin-3-yl)oxy)phenyl)amino)-7-ethoxyquinazolin-6-yl)-2-fluoro-4-(piperidin-1-yl)but-2-enamide (**8a**). The retention time of Z-isomer is 15.85 min; light-yellow solid; yield 33.2%. <sup>1</sup>H NMR (400 MHz, DMSO) δ 9.84 (s, 1H), 9.64 (s, 1H), 8.77 (s, 1H), 8.58 (s, 1H), 8.22 (s, 2H), 7.84 (dd, J = 8.8, 2.4 Hz, 1H), 7.31 (s, 1H), 7.27 (m, 2H), 7.21 (d, J = 8.8 Hz, 1H), 6.21 (dt, J = 36.8, 7.2 Hz, 1H), 4.28 (q, J = 6.8 Hz, 2H), 3.20 (d, J = 7.2 Hz, 2H), 2.45 (s, 3H), 2.39 (m, 4H), 1.52–1.41 (m, 9H). HRMS (ESI): *m/z* calcd for (C<sub>31</sub>H<sub>32</sub>ClFN<sub>6</sub>O<sub>3</sub> + H)<sup>+</sup>, 591.2286; found, 591.2266.

(E)-N-(4-((3-Chloro-4-((6-methylpyridin-3-yl)oxy)phenyl)amino)-7-ethoxyquinazolin-6-yl)-2-fluoro-4-(piperidin-1-yl)but-2-enamide (**8b**). The retention time of the E-isomer is 8.48 min; light-yellow solid; yield: 17.0%. <sup>1</sup>H NMR (400 MHz, DMSO) δ 9.84 (s, 1H), 8.77 (s, 1H), 8.58 (s, 1H), 8.21 (d, J = 2.8 Hz, 2H), 7.83 (d, J = 8.8 Hz, 1H), 7.31 (s, 1H), 7.27 (m, 2H), 7.20 (d, J = 8.4 Hz, 1H), 6.09 (dt, J = 23.6, 7.0 Hz, 1H), 4.32–4.26 (m, 2H), 3.45–3.44 (m, 2H), 2.45 (s, 3H), 2.40 (m, 4H), 1.49–1.41 (m, 9H). HRMS (ESI): *m/z* calcd for (C<sub>31</sub>H<sub>32</sub>ClFN<sub>6</sub>O<sub>3</sub> + H)<sup>+</sup>, 591.2286; found, 591.2280.

N-(4-((3-Chloro-4-(pyridin-2-ylmethoxy)phenyl)amino)-7-ethoxyquinazolin-6-yl)-2-fluoro-4-(piperidin-1-yl)but-2-enamide (**9a+9b**). The preparation was according to the compound (**1a+1b**). TLC R<sub>f</sub> = 0.52, 0.53 (DCM/MeOH = 10:1, the two isomers could be separated). The separation of the Z–E isomers was performed according to compound (**2a+2b**).

N-(4-((3-Chloro-4-((3-fluorobenzyl)oxy)phenyl)amino)-7-methoxyquinazolin-6-yl)-4-(dimethylamino)-2-fluorobut-2-enamide (**9a+9b**). The preparation was according to the compound (**1a+1b**). TLC R<sub>f</sub> = 0.53, 0.56 (DCM/MeOH = 10:1, the two isomers could be separated). The separation of the Z–E isomers was performed according to compound (**3a+3b**).

(Z)-N-(4-((3-Chloro-4-((3-fluorobenzyl)oxy)phenyl)amino)-7-methoxyquinazolin-6-yl)-4-(dimethylamino)-2-fluorobut-2-enamide (**9a**). The retention time of the Z-isomer is 8.61 min; light-yellow solid; yield 40.3%. <sup>1</sup>H NMR (400 MHz, DMSO) δ 9.75 (s, 1H), 9.69 (s, 1H), 8.68 (s, 1H), 8.53 (s, 1H), 7.99 (d, J = 2.8 Hz, 1H), 7.71 (dd, J = 9.2, 2.8 Hz, 1H), 7.50–7.44 (m, 1H), 7.34–7.30 (m, 3H), 7.25 (d, J = 9.2 Hz, 1H), 7.20–7.16 (m, 1H), 6.19 (dt, J = 36.0, 7.2 Hz, 1H), 5.25 (s, 2H), 3.99 (s, 3H), 3.18–3.15 (m, 2H), 2.19 (s, 6H). HRMS (ESI): *m/z* calcd for (C<sub>26</sub>H<sub>26</sub>ClF<sub>2</sub>N<sub>5</sub>O<sub>3</sub> + H)<sup>+</sup>, 554.1770; found, 554.1780.

(E)-N-(4-((3-Chloro-4-((3-fluorobenzyl)oxy)phenyl)amino)-7-methoxyquinazolin-6-yl)-4-(dimethylamino)-2-fluorobut-2-enamide (**9b**). The retention time of the E-isomer is 5.09 min; light-yellow solid; yield 21.7%. <sup>1</sup>H NMR (400 MHz, DMSO) δ 10.92 (s, 1H), 9.70 (s, 1H), 8.78 (s, 1H), 8.51 (s, 1H), 7.97 (d, J = 2.4 Hz, 1H), 7.69 (dd, J = 8.8, 2.8 Hz, 1H), 7.50–7.44 (m, 1H), 7.34–7.30 (m, 3H), 7.25 (d, J = 9.2 Hz, 1H), 7.21–7.16 (m, 1H), 6.11 (dt, J = 23.6, 6.8 Hz, 1H), 5.25 (s, 2H), 4.01 (s, 3H), 3.37 (s, 2H), 2.23 (s, 6H). HRMS (ESI): *m/z* calcd for (C<sub>26</sub>H<sub>26</sub>ClF<sub>2</sub>N<sub>5</sub>O<sub>3</sub> + H)<sup>+</sup>, 554.1770; found, 554.1784.

N-(4-((3-Chloro-4-((6-methylpyridin-3-yl)oxy)phenyl)amino)-7-ethoxyquinazolin-6-yl)-4-(dimethylamino)-2-fluorobut-2-enamide (**10a+10b**). The preparation was according to the compound (**1a+1b**). TLC R<sub>f</sub> = 0.52, 0.56 (DCM/MeOH = 10:1, the two isomers could be separated). The separation of the Z–E isomers was performed according to compound (**2a+2b**).

(Z)-N-(4-((3-Chloro-4-((6-methylpyridin-3-yl)oxy)phenyl)amino)-7-ethoxyquinazolin-6-yl)-4-(dimethylamino)-2-fluorobut-2-enamide (**10a**). The retention time of the Z-isomer is 5.77 min; light-yellow solid; yield 45%. <sup>1</sup>H NMR (400 MHz, DMSO) δ 9.84 (s, 1H), 9.63 (s, 1H), 8.78 (s, 1H), 8.57 (s, 1H), 8.25–8.21 (s, 2H), 7.84 (dd, J = 9.2, 2.4 Hz, 1H), 7.30 (s, 1H), 7.27–7.26 (m, 2H), 7.20 (d, J = 8.8 Hz, 1H), 6.20 (dt, J = 36.4, 7.2 Hz, 1H), 4.27 (q, J = 6.8 Hz, 2H), 2.45 (s,

3H), 2.19 (s, 6H), 1.42 (t,  $J = 6.8$  Hz, 3H). HRMS (ESI):  $m/z$  calcd for  $(C_{28}H_{28}ClFN_3O_3 + H)^+$ , 551.1973; found, 551.1983.

*(E)-N-(4-((3-Chloro-4-((6-methylpyridin-3-yl)oxy)phenyl)amino)-7-ethoxyquinazolin-6-yl)-4-(dimethylamino)-2-fluorobut-2-enamide (10b)*. The retention time of the *E*-isomer is 3.69 min; light-yellow solid; yield 24.3%.  $^1H$  NMR (400 MHz, DMSO)  $\delta$  9.84 (s, 1H), 8.81 (s, 1H), 8.56 (s, 1H), 8.22–8.20 (m, 2H), 7.83 (dd,  $J = 8.8, 2.4$  Hz, 1H), 7.30 (s, 1H), 7.27–7.26 (m, 2H), 7.20 (d,  $J = 8.8$  Hz, 1H), 6.11 (dt,  $J = 23.2, 7.2$  Hz, 1H), 4.29 (q,  $J = 6.8$  Hz, 2H), 2.45 (s, 3H), 2.22 (s, 6H), 1.43 (t,  $J = 6.8$  Hz, 3H). HRMS (ESI):  $m/z$  calcd for  $(C_{28}H_{28}ClFN_3O_3 + H)^+$ , 551.1973; found, 551.1988.

*N-(4-((3-Chloro-4-(cyclopropylmethoxy)phenyl)amino)-7-ethoxyquinazolin-6-yl)-4-(dimethylamino)-2-fluorobut-2-enamide (11a + 11b)*. The preparation was according to the compound (1a+1b). TLC  $R_f = 0.52, 0.53$  (DCM/MeOH = 10:1, the two isomers could be separated). The separation of the *Z*–*E* isomers were performed according to compound (2a+2b).

*(Z)-N-(4-((3-Chloro-4-(cyclopropylmethoxy)phenyl)amino)-7-ethoxyquinazolin-6-yl)-4-(dimethylamino)-2-fluorobut-2-enamide (11a)*. The retention time of the *Z*-isomer is 4.07 min; light-yellow solid; yield 43.4%.  $^1H$  NMR (400 MHz, DMSO)  $\delta$  9.69 (s, 1H), 9.65 (s, 1H), 8.74 (s, 1H), 8.51 (s, 1H), 7.96 (d,  $J = 2.4$  Hz, 1H), 7.69 (dd,  $J = 8.8, 2.4$  Hz, 1H), 7.28 (s, 1H), 7.15 (d,  $J = 8.8$  Hz, 1H), 6.20 (dt,  $J = 36.4, 7.2$  Hz, 1H), 4.27 (q,  $J = 7.2$  Hz, 2H), 3.92 (d,  $J = 6.8$  Hz, 2H), 3.18 (dd,  $J = 7.2, 2.0$  Hz, 2H), 2.20 (s, 6H), 1.42 (t,  $J = 7.2$  Hz, 3H), 1.12 (t,  $J = 7.2$  Hz, 1H), 0.63–0.56 (m, 2H), 0.39–0.33 (m, 2H). HRMS (ESI):  $m/z$  calcd for  $(C_{26}H_{29}ClFN_3O_3 + H)^+$ , 514.2021; found, 514.2017.

*(E)-N-(4-((3-Chloro-4-(cyclopropylmethoxy)phenyl)amino)-7-ethoxyquinazolin-6-yl)-4-(dimethylamino)-2-fluorobut-2-enamide (11b)*. The retention time of the *E*-isomer is 3.16 min; light-yellow solid; yield 26.6%.  $^1H$  NMR (400 MHz, DMSO)  $\delta$  10.52 (s, 1H), 9.69 (s, 1H), 8.77 (s, 1H), 8.50 (s, 1H), 7.94 (d,  $J = 2.4$  Hz, 1H), 7.68 (dd,  $J = 8.8, 2.4$  Hz, 1H), 7.28 (s, 1H), 7.15 (d,  $J = 9.2$  Hz, 1H), 6.12 (dt,  $J = 23.2, 6.8$  Hz, 1H), 4.28 (q,  $J = 7.0$  Hz, 2H), 3.92 (d,  $J = 6.8$  Hz, 2H), 3.37–3.38 (m, 2H), 2.22 (s, 6H), 1.43 (t,  $J = 7.2$  Hz, 3H), 1.27–1.24 (m, 1H), 0.66–0.56 (m, 2H), 0.37–0.36 (m, 2H). HRMS (ESI):  $m/z$  calcd for  $(C_{26}H_{29}ClFN_3O_3 + H)^+$ , 514.2021; found, 514.2017.

*N-(4-((3-Bromophenyl)amino)-7-methoxyquinazolin-6-yl)-4-(dimethylamino)-2-fluorobut-2-enamide (12a+12b)*. The preparation was according to the compound (1a+1b). TLC  $R_f = 0.52, 0.53$  (DCM/MeOH = 10:1, the two isomers could be separated). The separation of the *Z*–*E* isomers were performed according to compound (2a+2b).

*(Z)-N-(4-((3-Bromophenyl)amino)-7-methoxyquinazolin-6-yl)-4-(dimethylamino)-2-fluorobut-2-enamide (12a)*. The retention time of the *Z*-isomer is 7.40 min; light-yellow solid; yield 38.5%.  $^1H$  NMR (400 MHz, DMSO)  $\delta$  9.79 (s, 2H), 8.73 (s, 1H), 8.60 (s, 1H), 8.19 (t,  $J = 1.6$  Hz, 1H), 7.88 (d,  $J = 8.8$  Hz, 1H), 7.36–7.27 (m, 3H), 6.19 (dt,  $J = 36.4, 7.2$  Hz, 1H), 4.00 (s, 2H), 3.17 (dd,  $J = 7.2, 2.0$  Hz, 1H), 2.20 (s, 3H). HRMS (ESI):  $m/z$  calcd for  $(C_{21}H_{21}BrFN_3O_2 + H)^+$ , 474.0941; found, 476.0925.

*(E)-N-(4-((3-Bromophenyl)amino)-7-methoxyquinazolin-6-yl)-4-(dimethylamino)-2-fluorobut-2-enamide (12b)*. The retention time of the *E*-isomer is 5.19 min; light-yellow solid; yield 31.5%.  $^1H$  NMR (400 MHz, DMSO)  $\delta$  10.99 (s, 1H), 9.81 (s, 2H), 8.83 (s, 1H), 8.60 (s, 1H), 8.16 (s, 1H), 7.87 (d,  $J = 8.0$  Hz, 1H), 7.38–7.28 (m, 4H), 6.12 (td,  $J = 23.2, 6.8$  Hz, 1H), 4.02 (s, 3H), 3.27–3.25 (m, 2H), 2.22 (s, 6H). HRMS (ESI):  $m/z$  calcd for  $(C_{21}H_{21}BrFN_3O_2 + H)^+$ , 474.0941; found, 476.0925.

**Biological Section. Determination of the GSH Conjugates Addition to Substituted Olefins.** 1. *Determination of GSH Conjugation with N-Phenylacrylamide (A) or 2-Fluoro-N-phenylacrylamide (B)*. Reactions of *N*-phenylacrylamide (A) or 2-fluoro-*N*-phenylacrylamide (B) with GSH were monitored with an Agilent 1290 HPLC-6224 time-of-flight mass spectrometer. Reactions were initiated by mixing various volumes of the Michael acceptor (100 mM in ACN) with the GSH (1.0 M GSH in PBS, pH = 7.4). Final solutions in 200  $\mu$ L of PBS (Costar flat-bottom clear 96-well plate, 300  $\mu$ L per well), containing 1 mM Michael acceptor and increasing concentrations of GSH (10–200 mM), were incubated for 1440 min at room temp prior

to acquiring absorption spectra (214 nm). Formation of the thioether was quantified by area normalization method based on the peak area on HPLC spectrum. Data were fit using Excel to obtain equilibrium dissociation constants.

2. *Determination of GSH Conjugation with Compound 5a or Afatinib*. Test reactions of compound 5a or afatinib with GSH were also carried out. Reactions were initiated as described above by mixing equal volumes of compound 5a or afatinib (100 mM in ACN) with solutions of GSH (1 M in PBS, pH = 7.4). After incubation, conjugate reaction was observed at various time points (0–120 min) by an Agilent 1290 HPLC-6224 time-of-flight mass spectrometer.

*Cell Proliferation Assay*. The human epidermal carcinoma cell line A431 and human nonsmall cell lung cancer cell line NCI-H1975<sup>L858R/T790M</sup> were used to evaluate the potency of synthesized analogues in cell-based level. Both cell lines were purchased from American Type Culture Collection (ATCC). A431 was cultured with RPMI 1640 (GIBCO), and NCI-H1975<sup>L858R/T790M</sup> was cultured with Dulbecco's Modified Eagle's Medium (GIBCO). Both mediums were supplemented with penicillin, streptomycin, and 10% fetal bovine serum. The assays were performed using the CellTiter-Glo (Promega) Kit. A431 and NCI-H1975<sup>L858R/T790M</sup> cells were seeded in density of 2000 cells/well and 1500 cells/well, respectively, in 384-well plates (Corning) for 24 h. Duplicate wells were treated with test or reference compounds for 48 h at various concentrations or DMSO (Sigma) as control. Plates were incubated at 37 °C in 5% CO<sub>2</sub> atmosphere. Cell proliferation was measured according to the manufacturer's protocol. The IC<sub>50</sub> was calculated using GraphPad Prism 5.0.

*Kinase Inhibition Assay*. The assays were performed in vitro using the homogeneous time-resolved fluorescence (HTRF) method (Cisbio). EGFR was purchased from Sigma. The kinases and substrates were incubated first with synthesized analogues for 5 min in enzymatic buffer (for EGFR). Then ATP (Sigma) was added into the reaction mixture to start the enzyme reaction. The ATP concentrations used in each enzyme reaction were 1.65  $\mu$ M for EGFR, equivalent to the  $K_m$  of ATP for the corresponding enzyme in this assay condition. The assays were conducted at room temperature for 30 min and stopped by detection reagents which contain EDTA. The detection step lasted for 1 h. The IC<sub>50</sub> was calculated using GraphPad Prism 5.0.

*Microsomal Stability Assay*. All assays were conducted in single sample. The incubation mixtures were prepared in E-tube and were contained with 1  $\mu$ M test analogues, 0.5 mg/mL hepatic microsomes (from rat, mouse, dog, monkey, and human), and 1 mM NADPH in 100 mM potassium phosphate buffer solution (pH = 7.4). Reactions were initiated by the addition of NADPH and kept in a shaking water bath at 37 °C. After 0.5, 10, and 30 min incubations at 37 °C, the reactions were terminated by the addition of cold acetonitrile equivalent to the volume of the reaction mixture. The samples were vortexed for 10 min and then centrifuged at 10000 rpm for 10 min. The supernatant was subjected to LC/MS/MS (Waters UPLC/API4000 Q Trap). In the determination of the in vitro  $t_{1/2}$  (half-life, HL), the analyte peak areas were converted to percentage of drug remaining, using the  $T = 0$  peak area values as 100%. The slope of the linear regression from log percentage remaining versus incubation time relationships ( $-k$ ) was used in the conversion to the in vitro  $t_{1/2}$ , values by the in vitro  $t_{1/2} = -0.693/k$ . The percent remaining of test compound was calculated compared to the initial quantity at 0 time.

*Measurement of CYP Inhibition Assay*. Inhibition activity of CYP was evaluated by incubating 100  $\mu$ M human hepatic microsomes in the presence of 10  $\mu$ M test compound. The incubation mixture was allowed to stand for 20 min at 37 °C. The incubation was terminated by the addition of acetonitrile equivalent to the volume of the incubation mixture. After the centrifugation, the supernatant was subjected to LC/MS/MS (Waters UPLC/API4000 Q Trap). The relative CYP activity was calculated via the percentage of metabolite product.

*Pharmacokinetic Assay*. Male rats (Sprague–Dawley rats, body-weight range of 180–220 g, iv,  $n = 2$ , po,  $n = 3$ ) were administered analogue intravenously via the tail vein at 3 mg/kg, respectively, or orally at 10 mg/kg, respectively. At predetermined times 24 h or more

after dosing, 0.4 mL blood was collected and the plasma was separated by centrifugation (8000 rpm, 5 min, Sigma 3K15). The concentrations of the compound were measured in the plasma using LC/MS/MS after protein precipitation with acetonitrile. The relevant estimated pharmacokinetic parameters for plasma were derived using DAS 2.0.

**Mouse Tumor Xenograft Efficacy Study.** The efficacy study was conducted in strict accordance with protocols approved by the Institutional Animal Care and Use Committee of the Central Research Institute, Shanghai Pharmaceuticals Holding Co., Ltd. H1975 NSCLC xenografts were established by  $3.0 \times 10^7$  cells subcutaneously inoculated in nude mice. Treatments were initiated when tumors reached a mean group size of 50–150 mm<sup>3</sup>. The mice were randomized to Control (10 mL/kg 0.5% CMC-Na + 0.4% Tween80, ig administration), afatinib (30 mg/kg, ig administration), 2a (30 mg/kg, ig administration), 3a (30 mg/kg, ig administration), 5a (30 mg/kg, ig administration), 5a (60 mg/kg, ig administration), and 5a (15 mg/kg, ig administration) every 2 days for 9 days. The size of tumors were measured individually twice per week with microcalipers. Tumor volume (V) was calculated as  $V = (\text{length} \times \text{width})^2 / 2$ . The individual relative tumor volume (RTV) was calculated as follows:  $RTV = V_t / V_0$ , where  $V_t$  is the volume on each day of measurement and  $V_0$  is the volume on the day of initial treatment. Therapeutic effect of compound was expressed in terms of T/C% and the calculation formula is  $T/C (\%) = \text{mean RTV of the treated group} / \text{mean RTV of the control group} \times 100\%$ .

## ■ ASSOCIATED CONTENT

### Supporting Information

Additional figures and tables illustrating inhibition data, purity data, and <sup>1</sup>H NMR spectra. This material is available free of charge via the Internet at <http://pubs.acs.org>.

## ■ AUTHOR INFORMATION

### Corresponding Authors

\*For Y. Yu: phone, 86-571-8820 8452; fax, 86-571-8820 8452; E-mail, [yyu@zju.edu.cn](mailto:yyu@zju.edu.cn).

\*For J. Shen: E-mail, [jkshen@mail.shcnc.ac.cn](mailto:jkshen@mail.shcnc.ac.cn).

### Author Contributions

<sup>||</sup>Guangxin Xia and Wenteng Chen contributed equally to this work.

### Notes

The authors declare no competing financial interest.

## ■ ACKNOWLEDGMENTS

We thank Marc A. Giulianotti in Torrey Pines Institute for Molecular Studies, USA, for critical reading this manuscript and Xiaoming Xie in Shanghai Pharmaceutical Holding Co., Ltd., for performing NMR spectrometry for structure elucidation. This project was supported from the National Natural Science Foundation of China (no. 81273356), Program for Zhejiang Leading Team of S&T Innovation, and the Osteoporosis and Breast Cancer Research Center, USA, to Y. Yu, and the China Postdoctoral Science Foundation Funded Project (2014M550331) to W. Chen. We are also grateful for additional financial support from New Drug Creation Project of the National Science and Technology Major Foundation of China (no. 2010ZX09401-404) to Shanghai Pharmaceutical Holding Co., Ltd.

## ■ ABBREVIATIONS USED

Alk, anaplasticlymphoma kinase; EGFR, epidermal growth factor receptor; EGFR-TK, epidermal growth factor receptor tyrosine kinase; FLT, FMS like tyrosine kinase; GSH, glutathione; HER, human epidermal growth factor receptor;

hERG, human ether-a-go-go-related gene; JAK2, Janus kinase 2; NSCLC, nonsmall-cell lung cancer; PDGFR, platelet-derived growth factor receptor; SFC, supercritical fluid chromatography; Src, Rous sarcoma oncogene cellular homologue; SYK, spleen tyrosine kinase

## ■ REFERENCES

- (1) Yarden, Y.; Sliwkowski, M. X. Untangling the ErbB signalling network. *Nature Rev. Mol. Cell. Biol.* **2001**, *2*, 127–137.
- (2) Hynes, N. E.; Lane, H. A. ErbB receptors and cancer: the complexity of targeted inhibitors. *Nature Rev. Cancer* **2005**, *5*, 341–354.
- (3) Ciardiello, F.; Tortora, G. EGFR antagonists in cancer treatment. *N. Engl. J. Med.* **2008**, *358*, 1160–1174.
- (4) Roskoski, R., Jr. Anaplastic lymphoma kinase (ALK): structure, oncogenic activation, and pharmacological inhibition. *Pharmacol. Res.* **2013**, *68*, 68–94.
- (5) Maemondo, M.; Inoue, A.; Kobayashi, K.; Oizumi, S.; Isobe, H.; Saijo, Y.; Hagiwara, K.; Gemma, A.; Nukiwa, T.; Kudoh, S.; Kanazawa, M.; Nagao, K.; Nakai, Y.; Shibuya, M.; Akie, K.; Chonabayashi, N.; Hasegawa, Y.; Hayashibara, K.; Hino, M.; Hino, T.; Ikebuchi, K.; Ishii, Y.; Kaneko, N.; Kimura, Y.; Koba, H.; Kojima, T.; Kosahira, S.; Koyama, N.; Miki, H.; Minegishi, Y.; Morikawa, N.; Moriyama, G.; Murayama, Y.; Nagashima, M.; Niizuma, K.; Nitani, H.; Ogura, S.; Okamoto, Y.; Osaki, Y.; Sakai, H.; Sugita, H.; Suzuki, T.; Tanaka, J.; Tokunaga, H.; Tsukamoto, T.; Uematsu, K.; Usui, K.; Yasuda, K. Gefitinib or chemotherapy for non-small-cell lung cancer with mutated EGFR. *N. Engl. J. Med.* **2010**, *362*, 2380–2388.
- (6) Rosell, R.; Carcereny, E.; Gervais, R.; Vergnenegre, A.; Massuti, B.; Felip, E.; Palmero, R.; Garcia-Gomez, R.; Pallares, C.; Sanchez, J. M.; Porta, R.; Cobo, M.; Garrido, P.; Longo, F.; Moran, T.; Insa, A.; De Marinis, F.; Corre, R.; Bover, I.; Illiano, A.; Dansin, E.; de Castro, J.; Milella, M.; Reguart, N.; Altavilla, G.; Jimenez, U.; Provencio, M.; Moreno, M. A.; Terrasa, J.; Muñoz-Langa, J.; Valdivia, J.; Isla, D.; Domine, M.; Molinier, O.; Mazieres, J.; Baize, N.; Garcia-Campelo, R.; Robinet, G.; Rodriguez-Abreu, D.; Lopez-Vivanco, G.; Gebbia, V.; Ferrera-Delgado, L.; Bombard, P.; Bernabe, R.; Bearz, A.; Artal, A.; Cortesi, E.; Rolfo, C.; Sanchez-Ronco, M.; Drozdowskyj, A.; Queralt, C.; de Aguirre, I.; Ramirez, J. L.; Sanchez, J. J.; Molina, M. A.; Taron, M.; Paz-Ares, L. Spanish Lung Cancer Group in collaboration with Groupe Français de Pneumo-Cancérologie and Associazione Italiana Oncologia Toracica. Erlotinib versus standard chemotherapy as first-line treatment for European patients with advanced EGFR mutation-positive non-small-cell lung cancer (EURTAC): a multicentre, open-label, randomized phase 3 trial. *Lancet Oncol.* **2012**, *13*, 239–246.
- (7) Kobayashi, S.; Boggon, T. J.; Dayaram, T.; Jänne, P. A.; Kocher, O.; Meyerson, M.; Johnson, B. E.; Eck, M. J.; Tenen, D. G.; Halmos, B. EGFR mutation and resistance of non-small-cell lung cancer to gefitinib. *N. Engl. J. Med.* **2005**, *352*, 786–792.
- (8) Lee, J. K.; Shin, J. Y.; Kim, S.; Lee, S.; Park, C.; Kim, J. Y.; Koh, Y.; Keam, B.; Min, H. S.; Kim, T. M.; Jeon, Y. K.; Kim, D. W.; Chung, D. H.; Heo, D. S.; Lee, S. H.; Kim, J. I. Primary resistance to epidermal growth factor receptor (EGFR) tyrosine kinase inhibitors (TKIs) in patients with non-small-cell lung cancer harboring TKI-sensitive EGFR mutations: an exploratory study. *Ann. Oncol.* **2013**, *24*, 2080–2087.
- (9) Yun, C.-H.; Mengwasser, K. E.; Toms, A. V.; Woo, M. S.; Greulich, H.; Wong, K. K.; Meyerson, M.; Eck, M. J. The T790M mutation in EGFR kinase causes drug resistance by increasing the affinity for ATP. *Proc. Natl. Acad. Sci. U. S. A.* **2008**, *105*, 2070–2075.
- (10) Kwak, E. L.; Sordella, R.; Bell, D. W.; Godin-Heymann, N.; Okimoto, R. A.; Brannigan, B. W.; Harris, P. L.; Driscoll, D. R.; Fidias, P.; Lynch, T. J.; Rabindran, S. K.; McGinnis, J. P.; Wissner, A.; Sharma, S. V.; Isselbacher, K. J.; Settleman, J.; Haber, D. A. Irreversible inhibitors of the EGF receptor may circumvent acquired resistance to gefitinib. *Proc. Natl. Acad. Sci. U. S. A.* **2005**, *102*, 7665–7670.

(11) Bowles, D. W.; Weickhardt, A.; Jimeno, A. Afatinib for the treatment of patients with EGFR-positive non-small cell lung cancer. *Drugs Today* **2013**, *49*, 523–535.

(12) Wissner, A.; Overbeek, E.; Reich, M. F.; Brawner Floyd, M.; Johnson, B. D.; Mamuya, N.; Rosfjord, E. C.; Discifani, C.; Davis, R.; Shi, X.; Rabindran, S. K.; Gruber, B. C.; Ye, F.; Hallett, W. A.; Nilakantan, R.; Shen, R.; Wang, Y.-F.; Greenberger, L. M.; Tsou, H.-R. Synthesis and structure–activity relationships of 6, 7-disubstituted 4-anilinoquinoline-3-carbonitriles. The design of an orally active, irreversible inhibitor of the tyrosine kinase activity of the epidermal growth factor receptor (EGFR) and the human epidermal growth factor receptor-2 (HER-2). *J. Med. Chem.* **2003**, *46*, 49–63.

(13) Schwartz, P. A.; Kuzmic, P.; Solowiej, J.; Bergqvist, S.; Bolanos, B.; Almaden, C.; Nagata, A.; Ryan, K.; Feng, J.; Dalvie, D.; Kath, J. C.; Xu, M.; Wani, R.; Murray, B. M. Covalent EGFR inhibitor analysis reveals importance of reversible interactions to potency and mechanisms of drug resistance. *Proc. Natl. Acad. Sci. U. S. A.* **2014**, *111*, 173–178.

(14) (a) Serafimova, I. M.; Pufall, M. A.; Krishnan, S.; Duda, K.; Cohen, M. S.; Maglathlin, R. L.; McFarland, J. M.; Miller, R. M.; Frödin, M.; Taunton, J. Reversible targeting of noncatalytic cysteines with chemically tuned electrophiles. *Nature Chem. Biol.* **2012**, *8*, 471–476. (b) Miller, R. M.; Paavilainen, V. O.; Krishnan, S.; Serafimova, I. M.; Taunton, J. Electrophilic fragment-based design of reversible covalent kinase inhibitors. *J. Am. Soc. Chem.* **2013**, *135*, 5298–5301. (c) Nonoo, R. H.; Armstrong, A.; Mann, D. J. Kinetic template-guided tethering of fragments. *ChemMedChem* **2012**, *7*, 2082–2086.

(15) Bohm, H.-J.; Banner, D.; Bendels, S.; Kansy, M.; Kuhn, B.; Müller, K.; Obst-Sander, U.; Stahl, M. Fluorine in medicinal chemistry. *ChemBiolChem* **2004**, *5*, 637–643.

(16) Kirk, K. L. Fluorine in medicinal chemistry: recent therapeutic applications of fluorinated small molecules. *J. Fluorine Chem.* **2006**, *127*, 1013–1029.

(17) Hagmann, W. K. The many roles for fluorine in medicinal chemistry. *J. Med. Chem.* **2008**, *51*, 4359–4369.

(18) Ilardi, E. A.; Vitaku, E.; Njardarson, J. T. Data-mining for sulfur and fluorine: an evaluation of pharmaceuticals to reveal opportunities for drug design and discovery. *J. Med. Chem.* **2014**, *57*, 2832–2842.

(19) Rewcastle, G. W.; Palmer, B. D.; Bridges, A. J.; Showalter, H. D.; Sun, L.; Nelson, J.; McMichael, A.; Kraker, A. J.; Fry, D. W.; Denny, W. A. Tyrosine kinase inhibitors. 9. Synthesis and evaluation of fused tricyclic quinazoline analogues as ATP site inhibitors of the tyrosine kinase activity of the epidermal growth factor receptor. *J. Med. Chem.* **1996**, *39*, 918–928.

(20) Wu, J.; Chen, W.; Xia, G.; Zhang, J.; Shao, J.; Tan, B.; Zhang, C.; Yu, W.; Weng, Q.; Liu, H.; Hu, M.; Deng, H.; Hao, Y.; Shen, J.; Yu, Y. Design, synthesis, and biological evaluation of novel conformationally constrained inhibitors targeting EGFR. *ACS Med. Chem. Lett.* **2013**, *4*, 974–978.

(21) Kadjout, M.; Zemmouri, R.; Eddarir, S.; Rolando, C. An efficient access to (*Z*)- $\beta$ -fluoroallyl alcohols based on the two carbon homologation of aromatic aldehydes by Horner–Wadsworth–Emmons reaction with 2-(diethoxyphosphinyl)-2-fluoro-ethanethioic acid, *S*-ethyl ester followed by reduction with sodium borohydride. *Tetrahedron* **2012**, *68*, 3225–3230.

(22) Gansäuer, A.; Worgull, D.; Knebel, K.; Huth, I.; Schnakenburg, G. 4-Exo cyclizations by template. *Angew. Chem., Int. Ed.* **2009**, *48*, 8882–8885.

(23) Short, K. M.; Pham, S. M.; Williams, D. C.; Datta, S. Multisubstituted aromatic compounds as inhibitors of thrombin. WO 2011/126903, 2011.

(24) Barf, T.; Kaptein, A. Irreversible protein kinase inhibitors: balancing the benefits and risks. *J. Med. Chem.* **2012**, *55*, 6243–6644.

(25) Diaz, G. J.; Daniell, K.; Leitza, S. T.; Martin, R. L.; Su, Z.; McDermott, J. S.; Cox, B. F.; Gintant, G. A. The [<sup>3</sup>H]dofetilide binding assay is a predictive screening tool for hERG blockade and proarrhythmia: Comparison of intact cell and membrane preparations and effects of altering [K<sup>+</sup>]<sub>o</sub>. *J. Pharmacol. Toxicol. Methods* **2004**, *50*, 187–199.